eNeuro

Research Article: New Research | Disorders of the Nervous System

Beta frequency oscillations in the subthalamic nucleus are not sufficient for the development of symptoms of parkinsonian bradykinesia/ akinesia in rats

https://doi.org/10.1523/ENEURO.0089-19.2019

Cite as: eNeuro 2019; 10.1523/ENEURO.0089-19.2019

Received: 11 March 2019
Revised: 30 July 2019
Accepted: 11 September 2019

Beta frequency oscillations in the subthalamic nucleus are not sufficient for the development of symptoms of parkinsonian bradykinesia/akinesia in rats

Abbreviated title: Beta oscillations not sufficient for bradykinesia

Christina Behrend Swan[1,2], Derek J. Schulte[1], David T. Brocker[1], Warren M. Grill[1,3]

[1]Department of Biomedical Engineering, Duke University, Durham, NC 27708
[2]Duke University School of Medicine, Durham, NC 27710
[3]Departments of Neurobiology & Neurosurgery, Duke University Medical Center, Durham, NC 27710

Author contributions: CBS and WMG designed research; CBS and DJS performed research; DTB contributed analytic tools; CBS and DJS analyzed data; CBS and WMG wrote the paper.

Corresponding author:
Warren M. Grill, Email: warren.grill@duke.edu
Duke University, Department of Biomedical Engineering
Fitzpatrick CIEMAS, Room 1427
101 Science Drive, Box 90281
Durham, NC 27708-0281

Number of figures: 16
Number of tables: 9
Number of multimedia and 3D models: 0
Number of words for Abstract: 178
Number of words for Significance Statement: 66
Number of words for Introduction: 593
Number of words for Discussion: 2087

Acknowledgements:
The authors would like to thank Emily Shannon, Jaydeep Sambagni, and Jiashu Li for preparation of histological slides.

Conflict of Interest:
Christina Behrend Swan: I declare no competing financial interests.
David T. Brocker: I declare no competing financial interests.
Derek J. Schulte: I declare no competing financial interests.
Warren M. Grill: I declare no competing financial interests.

Funding sources:
This work was supported by NIH R37 NS040894, NIH R01 NS079312, Duke MSTP NIH T32 GM007171, and the Triangle Community Foundation.

ABSTRACT

Substantial correlative evidence links the synchronized, oscillatory patterns of neural activity that emerge in Parkinson's disease (PD) in the beta frequency range (13-30Hz) with bradykinesia in PD. However, conflicting evidence exists, and whether these changes in neural activity are causal of motor symptoms in PD remains unclear. We tested the hypothesis that the synchronized beta oscillations that emerge in PD are causal of symptoms of bradykinesia/akinesia. We designed patterns of stimulation that mimicked the temporal characteristics of single unit beta bursting activity seen in PD animals and humans. We applied these beta-patterned stimulation patterns along with continuous low and high frequency controls to the subthalamic nucleus (STN) of intact and 6-OHDA lesioned female Long-Evans and Sprague-Dawley rats. Beta-patterned paradigms were superior to low frequency controls at induction of beta power in downstream substantia nigra reticulata (SNr) neurons and in ipsilateral motor cortex. However, we did not detect deleterious effects on motor performance across a wide battery of validated behavioral tasks. Our results suggest that beta frequency oscillations may not be sufficient for the generation of bradykinesia/akinesia in PD.

SIGNIFICANCE STATEMENT

We explored whether a causal link exists between the synchronized, 13-30Hz (beta band) oscillations that emerge in Parkinson's disease (PD) and symptoms of bradykinesia/akinesia. The results provide not only for a better understanding of disease pathophysiology but also offers insights into the development of improved and novel

67 treatments for Parkinson's disease. Our study suggests that beta frequency oscillations
68 are not causally related to bradykinesia/akinesia in PD.
69
70 **INTRODUCTION**
71 The execution of voluntary movement relies on the coordinated generation,
72 refinement, and relay of neural signals by a network of cortical and subcortical
73 structures. In Parkinson's disease (PD) deterioration of the dopaminergic nigrostriatal
74 projection from death of substantia nigra compacta (SNc) neurons disrupts this network
75 and engenders symptoms of bradykinesia/akinesia, rigidity, rest tremor, and postural
76 instability (Dauer and Przedborski, 2003; Alves et al., 2008; Holtbernd and Eidelberg,
77 2012). Loss of nigral dopaminergic input to the striatum results in significant changes in
78 neural firing rates and patterns including increases in burst and oscillatory firing, as well
79 as excessive synchronization of firing within and across nuclei in the cortico-basal
80 ganglia loop (Brown et al., 2001; Levy et al., 2002; Kuhn et al., 2005). While the neural
81 mechanisms underlying the motor symptoms of PD are unknown, particular attention
82 has been given to synchronized, oscillatory neural activity occurring in a frequency band
83 of 13-30 Hz–termed the beta band–as these oscillations seem to be correlated with
84 symptoms of bradykinesia in PD (Kuhn et al., 2008). Indeed, treatments that improve
85 bradykinesia, including levodopa administration or deep brain stimulation (DBS), also
86 disrupt the beta band oscillations that are seen throughout the cortico-basal ganglia
87 loop, including in the subthalamic nucleus (STN) (Levy et al., 2002; Kuhn et al., 2006;
88 Kuhn et al., 2008; Dorval et al., 2010; Delaville et al., 2015). While the origin of beta
89 oscillatory activity in PD is still unknown, the STN (Plenz and Kital, 1999; Gatev et al.,

2006; Stein and Bar-Gad, 2013), the striatum (McCarthy et al., 2011) and the motor cortex (Yamawaki et al., 2008) have been postulated to be involved in the generation of beta band oscillations in PD. Regarding the STN, STN DBS at 20 Hz in PD patients reduced finger tapping rates (i.e., increased bradykinesia) as compared to 0 Hz and 50 Hz DBS (Chen et al., 2007). Such observations suggest a causal link between STN beta band oscillations and symptoms of bradykinesia and akinesia in PD. Conversely, animal models of PD demonstrated emergence of bradykinetic/akinetic symptoms prior to development of beta band oscillations (Degos et al., 2009). Chronic administration of a dopamine receptor blocker to intact rats resulted in an immediate increase in akinetic symptoms, but an increase in beta oscillatory power in primary sensorimotor cortex was not seen until the fourth day of treatment (Degos et al. 2009). If symptoms of bradykinesia/akinesia can be dissociated from beta band oscillations, these oscillations may be an epiphenomenon.

We tested the hypothesis that a causal relationship exists between STN beta band oscillations and symptoms of bradykinesia/akinesia in PD. We designed stimulation patterns to mimic the oscillatory burst firing seen in single STN neurons in human PD patients (Levy et al., 2002) and animal models of PD (Mallet et al., 2008). We applied these stimulation patterns to a biophysically-based computational model of the intact cortico-basal ganglia-thalamic loop (Kumaravelu et al., 2016) and assessed changes in beta power in the activity of model globus pallidus internus (GPi) neurons. We then applied the stimulation patterns to the STN of healthy (intact) and parkinsonian (lesioned) rats and quantified entrainment of downstream neurons and effects on motor performance. The stimulation patterns increased beta frequency power (BFP) in both

the computational model and healthy rats. However, we did not detect deleterious effects of the patterns on rat motor performance. Our findings challenge the notion of a causal link between STN beta band oscillations and symptoms of bradykinesia/akinesia in PD and suggest that STN beta band oscillations are not sufficient for the development of these symptoms in PD.

MATERIALS AND METHODS

We first applied patterns of stimulation confirmed to induce beta oscillatory power in a model cortico-basal ganglia circuit to the STN of intact rats. We used intact rats to apply our patterns to a 'naïve substrate,' as intact rats lack excessively synchronized endogenous beta oscillations that would confound any BFP generated by our patterns (Figure 1). In the second phase of our study we applied our patterns to 6-OHDA lesioned animals treated with levodopa doses titrated to disrupt endogenous BFP. The goal of this approach was to exploit the changes in circuit dynamics that occur in PD while controlling the source of BFP. The Duke University Institutional Animal Care and Use Committee approved all animal care and experimental procedures. Animals were housed in Duke University Division of Laboratory Animal Resources managed housing with unrestricted access to food and water except as detailed below for food reward-motivated behavioral tasks.

Chronic electrode implants

Anesthesia was induced in 10 female Long-Evans and 25 female Sprague-Dawley rats (250-350g) using a mixture of 7% sevoflurane and 2 L min^{-1} O_2 and maintained during surgery using 2.5-3.5% sevoflurane in 1-1.5 L min^{-1} O_2. Paw pinch

withdrawal, heart rate, and peripheral capillary oxygen saturation were monitored to ensure appropriate anesthetic depth. All cranial implants were performed using a Kopf stereotaxic frame with stereotaxic coordinates determined from a rat brain atlas (Paxinos and Watson 2005). Rats were implanted unilaterally with a 23-gauge cannula in the medial forebrain bundle (MFB) [from bregma: anterior-posterior (AP) -2.0 mm, medial-lateral (ML) ±2.0 mm; from brain surface: dorsal-ventral (DV) -7.0 mm]; a four-channel stimulating microelectrode array (MEA) in the STN [AP -3.6 mm, ML ±2.6 mm; from brain surface: DV: -6.8 to -7.2 mm]; and a 16-channel recording MEA in the substantia nigra reticulata (SNr) [AP -5.8 mm, ML ±2.3 mm; from brain surface: DV -6.8 to -7.2 mm]. The STN stimulating MEA was comprised of 2x2 75 µm 10 kΩ platinum-iridium (Pt-Ir) electrodes with an inter-electrode spacing of 300 µm (Microprobes for Life Science). Intra-operative recordings using a single 0.5 MΩ tungsten microelectrode were conducted to confirm the stereotaxic location of the STN prior to placement of the 2x2 MEA in the STN. The SNr recording MEA was comprised of 4x4 125 µm 0.5 MΩ Pt-Ir electrodes with inter-electrode spacing of 250 µm (Microprobes). Intra-operative recordings were performed as the 4x4 array was advanced to confirm the depth of SNr. All unilaterally placed implants were localized to the same hemisphere. Nine stainless steel bone screws were affixed to the skull. Three of these bone screws were placed over bilateral primary motor cortex (M1) [AP +2.5 mm, ML ±2.5 mm] and unilateral primary somatosensory cortex (S1) [AP -1.0 mm, ML 3.0 mm]. Electrocorticogram (ECoG) signals were measured by wiring these bone screws to an additional connector in the headcap. A bone screw over the cerebellar cortex served as a reference for

158 neural recordings. Dental acrylic was used to secure all implants to the bone screws.
159 Animals recovered for one week before any additional procedures were performed.

160 ***Stimulation parameters***

161 We designed different temporal patterns of electrical stimulation to mimic the
162 oscillatory burst firing seen in PD patients and parkinsonian animal models, including
163 both regular and irregular 'beta' bursting paradigms. We applied three regular and one
164 irregular beta bursting paradigms, low (15, 20, 25Hz) and high (225Hz) frequency
165 continuous stimulation patterns, which served as 'control' patterns to the bursting
166 paradigms, during behavioral tasks and neural recordings, yielding a total of eight
167 experimental stimulation patterns. The regular beta bursting paradigms were non-
168 varying patterns with fixed burst envelope frequency (BEF), intra-burst frequency (IBF),
169 and number of pulses per burst (Figure 1). We selected BEFs of 15, 20, and 25 Hz,
170 which corresponded approximately to the peak frequencies of beta oscillatory activity of
171 STN neurons seen in parkinsonian non-human primates (Moran et al., 2012), human
172 PD patients (Kuhn et al., 2008; Bronte-Stewart et al., 2009; Eusebio and Brown, 2009),
173 and 6-OHDA lesioned rats (Sharott et al., 2005), respectively. For each BEF we used
174 an IBF of 225 Hz and five pulses per burst based on analysis of published recordings of
175 STN single unit burst firing in PD patients (Levy et al., 2000; Levy et al., 2002). An IBF
176 of 225 Hz is consistent with intra-burst frequencies in STN neurons of PD patients,
177 which have been seen to range from 75 Hz to over 200 Hz (Birdno and Grill, 2008; Gale
178 et al., 2009; Welter et al., 2011).

179 We designed the irregular beta bursting paradigm through computational
180 optimization using a genetic algorithm (Brocker et al. 2017). The irregular beta bursting

paradigm was parameterized as a binary string. Each element represented a time bin of 1.5 ms. A '0' represented no stimulation and a '1' represented stimulation. The optimization objective was to determine the appropriate arrangement of 1s and 0s that maximized beta band oscillatory power in the firing of model GPi neurons in the computational model of the intact basal ganglia (see below). The fitness function was equal to the maximum power in the beta band of GPi neuron firings averaged over time and across GPi cells. The most 'fit' patterns were mated using fitness proportionate selection. The resulting stimulation train had a BEF of about 15 Hz, an IBF of about 700 Hz, a varying number of pulses per burst, and an average number of total pulses per second of 225 (Figure 1).

All stimulation patterns were comprised of charged-balanced, symmetric biphasic pulses of 90 μs/phase. MATLAB (R2009a, The MathWorks) was used to digitize stimulation pattern templates and drive a voltage-to-current stimulus isolator (A-M Systems). Bipolar stimulation was delivered through the stimulating MEA to the STN. Amplitudes for each animal ranged from 20-150 μA. The maximum stimulation amplitude chosen for each animal was the amplitude at a continuous stimulation frequency of 130 Hz that induced circling contralateral to the hemisphere to which stimulation was applied but minimized additional motor effects such as paw tremor or rearing. For behavioral studies, a single amplitude –the maximum determined for each animal– was applied for each stimulation pattern. For neural recording studies with stimulation, the applied amplitudes ranged from a sub-motor threshold amplitude, usually 20-25 uA, to the maximum amplitude determined for that animal. In summary, we applied eight stimulation patterns across a range of amplitudes during neural

recordings and a variety of behavioral tasks. Three regular bursting and one irregular bursting pattern were designed to mimic STN unit bursting activity seen in PD humans and rats. Three low frequency patterns matching the BEFs of the regular bursting patterns (15, 20, 25Hz) were applied to serve as controls that had beta spectral frequency but no bursts. A high frequency pattern matching the IBF of the regular bursting patterns (225Hz) was applied as an additional control.

Computational Model

The regular bursting, irregular bursting, and continuous frequency stimulation patterns were applied to the STN model neurons in a biophysically-based model of the cortico-basal ganglia-thalamic network (Kumaravelu et al. 2016). The model was comprised of a network of single compartment Hodgkin-Huxley type neurons representing regular spiking excitatory neurons and fast-spiking interneurons in cortex; direct (dopamine-type 1 receptor dominant) and indirect (dopamine-type 2 receptor dominant) medium spiny neurons of the striatum; STN; globus pallidus externus (GPe); GPi; and thalamic, and 59 cells of each cell type were included in the model. Multiple amplitudes were tested to span the range from no STN cell activation to activation of all model STN neurons. The pulse width of each monophasic pulse was fixed at 180 μs. Simulations were implemented in MATLAB R2014a with equations solved using the forward Euler method with a time step of 0.025 ms and a simulation length of 10 s (Kumaravelu et al., 2016).

The output measure was the peak power of beta band oscillatory activity averaged across all model GPi neurons. The averaged peak beta band power was calculated by first generating the average multi-taper spectrogram of the spike times of

all GPi neurons using Chronux (www.chronux.org) with MATLAB R2014a. A sliding window of 1 s and a step size of 0.1 s was used. Second, at each time point of the averaged spectrogram, the peak power between 13 and 30 Hz was extracted. Finally, all maximum power values across time were averaged to generate the average maximum beta band power for a given stimulation train pattern and amplitude.

Code Accessibility

Our model of the cortico-basal ganglia-thalamic network is available for download on Model DB, accession number 206232.

Behavioral tests prior to unilateral 6-OHDA lesion

Healthy (dopamine-intact) rats performed a variety of behavioral tasks after recovery from chronic electrode implantation to assess for induction of bradykinetic/akinetic symptoms by stimulation of the STN with any of the patterns. To mitigate that a single metric from one behavioral task may alone not be sensitive enough to detect stimulation induced symptoms, we used a constellation of previously validated quantitative behavioral outcomes. These tasks are widely used to assess the degree of bradykinetic/akinetic impairment in rodent models of PD, are sensitive to varying degrees of SNc dopaminergic cell loss, and should detect changes in motor function induced by applied beta-patterned stimulation paradigms. The stimulation patterns tested and the number of animals that performed each behavioral task are detailed in Table 1.

Bar test

The bar test detects forelimb akinesia, which develops prominently in the 6-OHDA rat model of PD with > 90% dopaminergic SNc cell loss (Duty and Jenner, 2011).

When placed in an abnormal upright posture with forelimbs gripping a bar typically 5-10 cm above the ground, 6-OHDA lesioned rats will take longer to release the bar than unlesioned rats (Duty and Jenner, 2011). The goal in utilizing this behavioral task was to determine if the unilaterally applied beta-patterned stimulation paradigms preferentially caused generation of contralateral forelimb bradykinetic or akinetic symptoms as compared to no stimulation and continuous stimulation controls. For this test, dopamine-intact animals were placed in a 36 cm x 24 cm clear plastic chamber with a 0.5 cm diameter bar 10 cm above the ground in a dim room. Animals received unilateral STN stimulation at the maximum amplitude determined for that animal. An experimental session alternated between blocks of no stimulation and blocks of stimulation such that each stimulation block was bracketed by a no stimulation block. Each block was comprised of 'pre-trial' and 'trial' periods. For a given block, the animal experienced a pre-trial period of three minutes of either no stimulation or a specific pattern of stimulation. After three minutes elapsed, the trial period began. If the block was a stimulation block, stimulation continued uninterrupted from the pre-trial period through the trial period. The animal was placed such that it was standing upright on its hind paws while its forepaws gripped the bar (Figure 6A). The total time each paw spent on the bar was measured as a function of stimulation paradigm. A trial ended after either three placements on the bar were quantified or 300 seconds elapsed. The order in which stimulation patterns were presented was randomized between experimental sessions. An experimental session lasted 1-2 hours depending on an animal's performance. For each animal, the total time each paw spent on the bar was averaged for each stimulation pattern. An increase in length of time on bar for the paw

contralateral to the stimulated hemisphere as compared to the ipsilateral paw and the no stimulation result was interpreted as generation of bradykinetic/akinetic symptoms.

Open field test

The open field test assesses spontaneous locomotor activity and is sensitive enough to discriminate between motor deficits caused by complete (> 90% SNc dopaminergic cell loss) and incomplete (~70% SNc dopaminergic cell loss) lesions in the 6-OHDA rat model of PD (Carvalho et al., 2013). 6-OHDA lesioned animals exhibit less motor activity than intact animals in an open field (Carvalho et al., 2013). The goal was to determine if unilaterally applied beta-patterned stimulation paradigms preferentially caused a decrease in movement speed or a decrease in the number of movement initiation episodes as compared to no stimulation and continuous stimulation controls. Dopamine-intact rats were placed in a dark 20 cm diameter cylinder, and an infrared camera captured all movements (Figure 7A). Animals received unilateral STN stimulation at the maximum amplitude determined for that animal. An experimental session alternated between blocks of no stimulation and blocks of stimulation such that each stimulation block was bracketed by a no stimulation block. Each block was three minutes long. An experimental session was limited to 60 minutes to minimize overall experiment duration. As such, during each experimental session, 1-2 beta bursting paradigms in addition to the corresponding low and high frequency continuous control patterns were applied. Additional experimental sessions were performed after a rest period of ~5-7 days to avoid habituation of the animal to the chamber. The order in which stimulation patterns were presented was re-randomized between experimental sessions. Videos were analyzed using TopScan Version 2.0 (CleverSystems, Inc.) and

296 MATLAB. Average linear speed, average number of pauses per second, and average
297 pause length were measured, and results were normalized for each animal to the no
298 stimulation results to facilitate comparison across animals. A significant decrease in
299 average linear speed and a significant increase in average pause length and average
300 number of pauses per second as compared to the no stimulation results was interpreted
301 as generation of bradykinesia/akinesia.

302 ***Adjusting steps test***

303 The adjusting steps test assesses forelimb akinesia in dopamine-depleted rats
304 and can detect a forelimb motor deficit at a striatal dopamine depletion levels of 80% or
305 greater (Chang et al., 1999). When suspended vertically such that the body weight is
306 supported by the forelimbs, a 6-OHDA lesioned rat will drag its affected forelimb rather
307 than making adjusting steps to support its weight when dragged backwards or laterally
308 (Chang et al., 1999; Fleming, 2009; Glajch et al., 2012). The goal was to determine if
309 unilaterally applied beta-patterned stimulation paradigms preferentially caused an
310 increase in akinesia in the contralateral forelimb as compared to no stimulation and
311 continuous stimulation controls. Dopamine-intact rats were gripped around the hips to
312 immobilize the hindlimbs and suspended vertically on a 77 cm x 16 cm glass plank such
313 that the animal supported its weight through its forepaws (Figure 8A). A video camera
314 positioned below the glass plank recorded all forelimb movements. Animals were
315 dragged backwards, and the number of backward steps the animal made with each
316 forepaw along the length of the glass plank was recorded. The animal performed 3-5
317 trials of this task. The animal then was returned to its home cage and received unilateral
318 STN stimulation at the maximum amplitude determined for that animal for 5 minutes.

While STN stimulation continued, each animal performed 3-5 additional trials of this task. A single pattern of stimulation was applied during an experimental session, which typically lasted 30 minutes, and animals were given at least three hours of rest in between experimental sessions. A decrease in forelimb adjusting steps for the forelimb contralateral to the stimulated hemisphere as compared to the ipsilateral forelimb and the no stimulation result was interpreted as generation of bradykinesia/akinesia.

Forelimb use asymmetry test

The forelimb use asymmetry test assesses forelimb akinesia in dopamine-depleted rats, and performance in this task correlates with the amount of striatal dopamine depletion (Connor et al., 1999; Fleming, 2009). When placed in a narrow cylinder, 6-OHDA lesioned rats will avoid using the affected forelimb during vertical exploration of the cylinder (Schallert et al., 2000; Fleming, 2009). The goal was to determine if unilaterally applied beta-patterned stimulation paradigms preferentially caused a decrease in limb use preference in the contralateral forelimb during vertical exploration as compared to no stimulation and continuous stimulation controls. Dopamine-intact rats were placed in their home cage for one hour in a dark room to acclimate to the environment. After one hour, rats received either no stimulation or unilateral STN stimulation with a single pattern for five minutes. Rats were then placed in a 20 cm diameter x 30 cm high clear cylinder for 5-10 minutes (Figure 9A). If stimulation was applied in a given experimental session, it continued for the full duration of the task. Animals were videotaped during the task, and mirrors were used to capture a 360° view of animal exploration of the cylinder. During rears the numbers of single and bilateral forepaw touches to the cylinder wall were quantified. Additionally, upon

342 descending from a rear, the rat's preference for using one or both forepaws to support
343 its weight was quantified. Animals were given 7 days of rest between experimental
344 sessions to diminish habituation to the cylinder. A decrease in use of the forelimb
345 contralateral to the stimulated hemisphere on vertical exploration and landings as
346 compared to the ipsilateral forelimb and the no stimulation result was interpreted as
347 generation of bradykinesia/akinesia.

348 ***Skilled forelimb reaching test***

349 A skilled forelimb reaching task was conducted using the Vulintus MotoTrak
350 System (Hays et al., 2013). Animals were placed in a 36 cm x 24 cm x 16 cm acrylic
351 chamber with a narrow slot at one end positioned so as to restrict performance to a
352 specific forelimb. A lever on a motorized track was positioned at or just outside of the
353 slot, and animals were trained to depress the lever twice within a certain time window to
354 receive a food reward (Figure 10A). Impaired animals demonstrate longer inter-press
355 intervals, fewer presses per trials, and fewer successes (Hays et al., 2013).

356 The goal was to determine if unilaterally applied beta-patterned stimulation
357 preferentially caused impairment in the forelimb contralateral to the stimulated
358 hemisphere during lever presses as compared to no stimulation and continuous
359 stimulation controls. Dopamine-intact rats were restricted to 12 g of food per day until
360 their body weight was between 85-90% of their free feeding weight. During an
361 experimental session, a rat was placed in its home cage in a dark room and received
362 unilateral STN stimulation at the maximum amplitude determined for that animal for 5
363 minutes. The rat then was placed in the experimental chamber while stimulation
364 continued. The animal was allowed thirty minutes in the experimental chamber to

perform the task. A successful trial was defined as two lever presses within a 0.5 sec window with the lever positioned 1.0 cm outside of the chamber. Inter-press interval, mean press duration, initiation of press to hit peak latency, and success rate to a successful trial were calculated. A maximum of two experimental sessions were performed per day, and animals rested for at least three hours between sessions. Sessions without stimulation were conducted on an identical timeline to those with stimulation. An increase in inter-press interval, mean press duration, and initiation of press to hit peak latency and a decrease in success rate were interpreted as generation of bradykinesia/akinesia.

6-OHDA lesioning

Eleven animals were rendered hemi-parkinsonian through unilateral administration of the neurotoxin 6-hydroxydopamine hydrobromide (6-OHDA, Sigma-Aldrich) via the MFB cannula to evoke unilateral degeneration of dopaminergic neurons in the nigrostriatal pathway (Tieu, 2011). As 6-OHDA also will selectively destroy noradrenergic neurons, thirty minutes prior to 6-OHDA administration animals were pre-treated with intraperitoneal (i.p.) injections of 5mg/kg desipramine (Sigma-Aldrich) to protect nonadrenergic neurons and 50mg/kg pargyline (Sigma-Aldrich) to inhibit monoamine oxidase activity (McConnell et al., 2012; So et al., 2012). Anesthesia was induced using a mixture of 7 % sevoflurane in 2 L min^{-1} O_2 and maintained using 2.5-3.5 % sevoflurane in 1-1.5 L min^{-1} O_2. Animals were positioned in a Kopf stereotactic frame for intra-cerebral injection. Immediately prior to infusion, 5mg 6-OHDA was dissolved into 2 mL 0.02% ascorbic saline (Sigma-Aldrich) stored at 4°C to produce a final concentration of 10 mM. Ten microliters of 6-OHDA solution was administered through

388 the MFB cannula using a Hamilton syringe at a rate of 2 µL/min. Animals were given
389 one week to recover. Animals that did not exhibit unilateral motor symptoms after the
390 recovery period were re-infused with 6-OHDA a maximum of two additional times.

391 ***Methamphetamine-induced circling test***

392 One week after injection of 6-OHDA, each rat was injected with a
393 methamphetamine solution (Sigma-Aldrich) at a concentration of 1.5-2.5 mg/kg i.p. and
394 placed in a 20 cm diameter x 30 cm high cylinder within a dark chamber. Animals with
395 severe unilateral lesions of dopaminergic pathways will circle ipsilateral to the lesion
396 after administration of methamphetamine (Ungerstedt and Arbuthnott, 1970). The
397 activity of the animal was monitored using an infrared lamp and camera for two hours,
398 and during this time blocks of high frequency stimulation were applied for 60 s with 120
399 s of rest between each stimulation pattern (McConnell et al., 2012). TopScan Version
400 2.0. was used to determine the position of each animal within the cylinder for each video
401 frame. From this information, the angular velocity of each animal with and without
402 stimulation was calculated using MATLAB. Based on previous histological analysis,
403 animals that circled at a rate of at least 3 turns/min with no stimulation were deemed to
404 have had greater than 90 % loss of dopaminergic neurons in the SNc (Fang et al., 2006;
405 So et al., 2012; Ungerstedt and Arbuthnott, 1970), which was defined as a successful
406 lesioning procedure. Animals that did not meet this criterion were re-lesioned up to two
407 additional times.

408 ***Post-lesion behavioral positive controls***

409 After confirmation of successful lesion via the methamphetamine-induced circling
410 test, baseline performance and performance with continuous 130 Hz stimulation were

assessed in the bar test, the open field test, the adjusting steps test, the forelimb use asymmetry test, and the skilled forelimb reaching test. The amplitude for 130 Hz stimulation was consistent with that used for each animal before the lesioning procedure. Assessing motor performance under these conditions provided a threshold for generation of parkinsonian symptoms through use of beta-patterned stimulation for each behavioral task. The number of animals that performed each positive control task can be found in Table 1.

Post-lesion beta-patterned stimulation behavioral assessments

Rats were pre-treated with 15 mg/kg of benserazide hydrochloride (i.p., Sigma-Aldrich), a peripheral DOPA decarboxylase inhibitor, and L-3,4-dihydroxyphenylalanine methyl ester hydrochloride (levodopa) (15-19 mg/kg, i.p., Sigma-Aldrich). Doses of levodopa were selected for each animal that disrupted cortical M1 power ipsilateral to the lesion (see below) but did not make the animal dyskinetic. The adjusting steps test and the skilled forelimb reaching task were administered to assess performance for a drug only baseline and during beta-patterned and control stimulation. The patterns assessed are detailed in Table 1.

Neuronal recordings

Sixteen single unit channels were recorded from the SNr, and three ECoG channels–M1 bilaterally and S1 from the hemisphere contralateral to STN implant–were recorded simultaneously using a multichannel acquisition processor system (Plexon, Inc.). The rat was placed in an open top chamber within a Faraday cage, and recordings were performed while the rat was awake and freely roaming the chamber. The three ECoG channels were also recorded after 6-OHDA lesion and used to titrate doses of

434 levodopa as described below. The voltage signal used to drive the stimulus isolator was
435 recorded simultaneously with the neural signals on an analog input channel to enable
436 precise time-locking of the stimulation input to the neural recordings in subsequent
437 analyses. For single unit recordings gain and filter settings were: gain = 20000, filter =
438 150Hz-8.8kHz, sampling rate = 40kHz, and for LFP recordings, gain and filter settings
439 were: gain = 2500-5000, filter = 150Hz-8.8kHz, sampling rate = 20kHz.

440 *Neuronal recordings prior to unilateral 6-OHDA lesion*

441 Recording sessions were 3-4 hours in length, and all patterns listed in Table 1
442 were applied during an experimental session. A single pattern block consisted of 90-120
443 s of no stimulation, 90-120 s of applied stimulation, and 90-120 s of no stimulation while
444 single units were recorded from SNr. ECoG also was recorded simultaneously from
445 bilateral M1 and contralateral S1. Each pattern was applied at 3-4 amplitudes, ranging
446 from 25uA to the highest tolerated amplitude for each animal. The order in which
447 patterns and amplitudes were presented was randomized. Each animal participated in
448 up to four recording sessions. Pattern and amplitude presentation were re-randomized
449 between sessions.

450 ***Neuronal recordings after unilateral 6-OHDA lesion***

451 Two types of recording sessions were conducted. Although unilateral motor
452 impairment can be detected shortly after 6-OHDA lesion increases in BFP appear to
453 emerge after presentation of motor symptoms (Degos et al., 2009). We were able to
454 detect beta frequency peaks in ipsilateral M1 ECoG approximately three weeks post-
455 lesion (Figure 2A). Prior to emergence of this peak, stimulation and SNr unit recording
456 sessions were performed in a manner identical to the recordings done in intact rats.

Each animal participated in up to two experimental sessions. Pattern and amplitude were re-randomized between experimental sessions.

After emergence of a beta peak in ipsilateral M1 ECoG, different doses of levodopa were administered during different recording sessions until sustained depression of ipsilateral M1 BFP was observed (Figure 2B). As peak drug effect in the rat lasts approximately two hours (Putterman et al., 2007), stimulation and SNr unit recording sessions then proceeded as without drug pre-treatment but were executed only at the maximum amplitude to allow for all patterns to be applied within the same recording session.

Single unit recording analysis

Single units were sorted online using SortClient and were classified further using Offline Sorter (Plexon, Inc.). Timestamps of unit activity were imported into MATLAB for analysis. Inter-spike interval (ISI) histograms of unit activity were calculated for the baseline and stimulation periods. Artifact timestamps were extracted from the recorded voltage input signal and used to calculate inter-pulse interval (IPI) histograms and peri-stimulus time histograms (PSTH). A virtual PSTH was calculated for the pre-stimulation time period by shifting the artifact timestamps to align with the beginning of the pre-stimulation recording period. Blanking periods of 0.7 ms before through 2 ms after the artifact timestamp were applied to eliminate the possibility of a portion of the artifact waveform being counted as a unit timestamp. These blanking periods were applied to the virtual PSTHs, as well. For burst stimulation patterns, PSTHs were aligned to the last pulse in each burst to assess activity in the inter-burst interval. A bin width of 0.2 s was used to generate the bin axes for both virtual and stimulation PSTHs. The change

480 in unit activity from pre-stimulation baseline was determined by transforming the
481 stimulation PSTH bin counts to z-scores relative to the virtual PSTH bin counts
482 according to the following formula, where *i* represents a single stimulation PSTH bin
483 value:

$$Z_{stim}(i)=\frac{(PSTH_{stim}(i) - \overline{PSTH_{virtual}})}{\sigma_{virtual}}$$

484 A threshold of four standard deviations from the mean ($Z_{stim}(i) \geq 4$, $p < 0.001$) was
485 chosen to distinguish strong, statistically significant changes in unit activity from the pre-
486 stimulation baseline in the normalized stimulation PSTH (Figure 3).

487 To determine if single unit activity in the SNr was entrained to stimulation in the
488 STN, the excitatory effective pulse fraction (eEPF) was calculated using the normalized
489 PSTH (Agnesi et al., 2015). The effective pulse fraction (EPF) is a ratio (range: 0-1) that
490 relates the number of single unit firings evoked by a stimulus pulse at a consistent
491 latency within the inter-pulse interval (IPI) to the number of unit firings evoked by a
492 'virtual' stimulus pulse at the same latency during a baseline period. This latency within
493 the inter-pulse interval is referred to as a phase and represents at least two consecutive
494 time bins with a statistically significant increase in single unit activity from the baseline
495 period. The excitatory effective pulse fraction was designed for a stimulation site and
496 recording site linked by a glutamatergic monosynaptic projection, as are the STN and
497 SNr, and is calculated as follows for each identified IPI phase (Agnesi et al., 2015):

$$eEPF = \frac{pfs\text{-}pfsb}{\text{number of stimulus pulses}\text{-}pfsb}$$

498 where pfs represents the number of stimuli during the stimulation period followed by a
499 single unit spike and pfsb represents the number of shifted stimulus pulses followed by

a single unit spike during the pre-stimulation period. An eEPF was calculated for all distinct IPI phases of the normalized stimulation PSTH with statistically significant increases in unit activity from the pre-stimulation period (Figure 3). If multiple distinct IPI phases were present in a single normalized stimulation PSTH, then the eEPFs for these phases were averaged to assess the overall effect of stimulation pattern and amplitude.

The change in beta-frequency power in SNr unit activity as a result of STN stimulation was quantified through calculation of multi-taper spectra using the Chronux data package for MATLAB. Spectra were calculated for both the pre-stimulation and stimulation time periods using averaging over 15-20 s windows (6 time segments per recording period), five slepian data tapers, a bandpass range of 1-58 Hz, and 0.04 Hz frequency resolution. To account for the effect of amplifier blanking, an individualized blanking period was determined for each unit. Using the lowest amplitude stimulation recording for each unit, a PSTH was created without pre-determined blanking and the length of time between a stimulation pulse and the first unit spike was found. This individualized blanking period was then imposed on the pre-stimulation recording for each unit; any spikes occurring within this time period following a virtual pulse were deleted. These blanking periods ranged from 0.6-2 ms and avoided introduction of artificial BFP into the spectra. After calculation of pre- and during stimulation spectra, the percent of total power in the beta band was quantified. Each power value was divided by the sum of all power values to convert it to a fraction of total power. The percent of total power in the beta band was then equal to the sum of each scaled power value in the range of 13 - 30 Hz. The difference between the percent of total power in

522 the beta band with and without stimulation for each amplitude, frequency pattern, and
523 single unit was determined.

524 ***Electrocorticogram recording analysis***

525 Three ECoG channels–bilateral M1 and S1 contralateral to the implanted STN–
526 were recorded during stimulation in ten intact animals. Our goal was to quantify the
527 amount of BFP induced by stimulation in ipsilateral M1 ECoG given the connections
528 between STN and motor cortex (Gatev et al., 2006; Delaville et al., 2015). While
529 projections between ipsilateral primary somatosensory cortex and STN have been
530 identified in the rat, contralateral projections have not been identified (Canteras et al.,
531 1988). To distinguish inducement of physiological beta power from the effect of
532 stimulation artifact, the effects seen in ipsilateral M1 ECoG were referenced to
533 contralateral S1 ECoG data as described below.

534 Ipsilateral M1 and contralateral S1 continuous data were imported into MATLAB
535 and divided into pre-stimulation and with stimulation segments. ECoG segments
536 recorded during stimulation were high-pass filtered using a three-pole Butterworth filter
537 with a 2 Hz cutoff frequency. Stimulus artifacts were digitally blanked via linear
538 interpolation from 0.1 ms to 1.5 ms after the start of a stimulus pulse. The data were
539 then divided into segments of repeating IPIs and averaged to determine an average
540 evoked response to stimulation. This average evoked response was subtracted from the
541 overall dataset to reduce spectral power at the stimulation frequencies (Brocker et al.,
542 2017). Finally, the data again were band-pass filtered using a three-pole Butterworth
543 filter between 2-100 Hz. ECoG segments recorded prior to stimulation underwent only
544 both rounds of filtering.

Multi-taper spectra were calculated for ipsilateral M1 and contralateral S1 ECoG channels for both pre-stimulation and during stimulation time segments. Spectra were calculated using averaging over 5 sec windows, three slepian data tapers, and a bandpass range of 3-55 Hz. As with the single unit spectra, the percent of total power in the beta band was quantified for both pre-stimulation and during stimulation spectra. The difference between the percent of total power in the beta band with and without stimulation for each amplitude and stimulation pattern was calculated for both ipsilateral M1 and contralateral S1 spectra. Finally, the percent of total power in the beta band during stimulation for contralateral S1 ECoG was subtracted from the percent of total power in the beta band during stimulation for ipsilateral M1 ECoG (Figure 14).

Histology

Histological analysis was conducted to determine the location of all implanted electrode arrays as well as the extent of the 6-OHDA lesion. Each animal was deeply anesthetized with urethane (1.8 g/kg, i.p.) and transcardially perfused with cold phosphate-buffered saline (PBS) followed by 10 % formalin. The head was removed and post-fixed in 10 % formalin overnight at 4 °C. The following day the brain was removed and placed in a 30% sucrose solution and stored at 4 °C until it sank, usually about 48 h. The left hemisphere was dyed to assist in hemispherical identification of brain slices. Brains were then placed in optimal cutting temperature compound (OCT, Tissue Tek) and frozen to -80 °C. A cryostat at approximately -20 °C was used to cut 50 µm serial coronal slices.

To identify implanted electrode tip locations, a cresyl violet stain was used. Brain slices were rinsed in PBS, mounted onto microscope slides, and left to dry overnight.

Mounted slices were de-fatted by placing slides in forward and then backward through a series of solutions for three minutes each: distilled water, 70 % ethanol, 95 % ethanol x 2, 100 % ethanol x 2, Histoclear x 2. Slides were then stained in a 0.1 % cresyl violet solution (Sigma-Aldrich) for ~30 minutes, dried and coverslipped. Slides were visually inspected using a light microscope to locate electrode tips. Rats were excluded from analysis if stimulating electrode tips were not located within the STN (Figure 4).

To visualize the extent of the 6-OHDA lesion, a fluorescent immunostaining protocol was used. Slices were rinsed three times in a 1X PBS solution and incubated for one hour at 4°C in a 1X PBS-based solution containing 8 % normal goat serum (Jackson ImmunoResearch) and 1 % Triton-X (VWR). Slices were rinsed three times in 1X PBS for 5 minutes each and then incubated overnight at 4°C in a primary 1X PBS-based solution containing 2 % normal goat serum and 0.2 % anti-tyrosine hydroxylase (anti-TH; monoclonal mouse IgG1; 1:500; Sigma-Aldrich). Slices were again rinsed three times in 1X PBS for 5 minutes each and then incubated for 1 h in a secondary 1X PBS-based solution containing 2 % normal goat serum, 0.5 % Triton-X, and 0.2 % Alexa Fluor 594 goat anti-mouse IgG1 (Life Technologies). Slices were then rinsed three times in 1X PBS for 5 minutes each and coverslipped with SouthernBiotech DAPI-Fluoromount-G (Fisher Scientific).

Experimental Design and Statistical Analyses

All animal data are expressed as mean ± SE with *n* = the number of animals and reported for each behavioral test in Table 1. To determine significance in behavioral performance metrics, animal data were analyzed using RMANOVA, unpaired t-tests, and paired t-tests as appropriate with fixed factors including paw, pattern, amplitude,

591 lesion state, and/or drug state depending on the particular behavior test and animal ID
592 as the random variable. The Shapiro-Wilk test was used to test normality of the data,
593 which was found to be normal or near normal. Given the robustness of ANOVA both to
594 distributions with significant departures from normality and to small sample sizes
595 (Blanca et al., 2017, Normal, 2010, Pearson, 1931), we used parametric statistics for
596 the majority of our data. Wilcoxon rank sum tests were used to analyze censored data
597 (bar test). Interpretation of the effects of stimulation on neural data was made using
598 ANOVA with fixed factors including pattern, amplitude, lesion state, and/or drug state as
599 appropriate. Where ANOVAs and RMANOVAs were found to be significant, *post hoc*
600 tests to distinguish differences among factor levels were the Student's t-test if a factor
601 had only two levels or the Tukey's honest significant difference (HSD) if a factor had
602 greater than two levels. The alpha level chosen for statistical significance was 0.05.
603
604 **RESULTS**
605 ***Histological Analysis of Electrode Locations and 6-OHDA Lesions***
606 Verification of stimulation electrode tip locations in STN is shown in Figure 4.
607 Only animals with electrode tips located in the STN were included in behavioral and
608 neural analyses. For 3/35 animals, brains were not available for histological processing.
609 Previously recorded videos of behavioral response to 130 Hz stimulation were used to
610 determine whether to include these animals in subsequent analyses, as a contralateral
611 turning response to high frequency stimulation correlates very strongly with successful
612 targeting of the STN (So et al., 2012).

Effects of Beta-Patterned Stimulation: Model Cortico-Basal Ganglia-Thalamic Loop

The amount of beta band power in the 'healthy' model cortico-basal ganglia-thalamic loop was affected by stimulation pattern and the fraction of total cells activated with a significant interaction between pattern and fraction of cells activated (Figure 5G); statistics are reported in Figure 5 and **Table 2**. While some BFP was present in the model network in the healthy state (Figure 5G), beta bursting rhythms were not present in the STN or GPi cell populations (Figure 5A, Figure 5C-D). When beta patterned stimulation was applied to model STN neurons, beta band rhythms were seen in model STN and GPi neurons (Figure 5B, Figure 5E-F). Post-hoc testing revealed that while continuous low frequency stimulation paradigms at beta band frequencies did increase averaged peak beta band power, irregular and regular beta stimulation paradigms increased beta band power beyond that generated by continuous low frequency stimulation (Figure 5G). Also, continuous high frequency stimulation suppressed power in the beta band with increasing STN neuron activation as compared to the 'healthy' model baseline and the 'PD' model baseline (Figure 5G). After confirming generation of BFP in the computational model, these same patterns were applied to healthy rats to quantify any resulting deteriorations in motor performance as well as to document an increase in BFP in SNr unit activity.

Effects of beta-patterned STN stimulation on behavior in healthy rats

We administered five widely used motor tasks to maximize our ability to detect induction of bradykinesia/akinesia due to beta-patterned stimulation. Although most of these tasks were sensitive to differences in performance between intact and 6-OHDA

lesioned rats, we did not detect stimulation-induced deteriorations in motor performance in healthy rats.

Bar test

Forelimb akinesia as assessed by length of time on the bar was unaffected by beta-patterned stimulation (**Table 3**, Figure 6). Use of the bar test detected a statistically significant worsening of forelimb akinesia after treatment with 6-OHDA that was improved by 130 Hz STN stimulation (Figure 6B). However, we detected no differences in performance between beta-patterned, continuous low frequency, or continuous high frequency paradigms in intact animals as compared to the no stimulation condition (Figure 6B). There also was no impact of paw on the results nor a significant interaction between pattern and paw (Figure 6B).

Open field test

The open field test did not detect differences in locomotor activity across stimulation paradigms (Table 4, Figure 7). Beta-patterned, continuous low frequency, and continuous high frequency paradigms did not evoke discernable differences in linear speed (Figure 7B), number of pauses per second (Figure 7C), or pause length (Figure 7D) in intact animals as compared to the no stimulation condition. However, 6-OHDA treated animal performance also did not differ significantly from intact animal performance either at baseline or during 130 Hz STN stimulation (Figure 7B-D). The average linear speed during the no stimulation condition was only 7 mm/sec (Figure 7B) implying that animals were not exploring the arena during the experiment, thus making it difficult to detect differences in activity across patterns or lesion states.

Adjusting steps test

Forelimb akinesia as assessed by the adjusting steps test was not appreciably different with beta-patterned, continuous low frequency, or continuous high frequency stimulation in intact animals as compared to the no stimulation condition (**Table 5**, Figure 8). There was no impact of paw on the intact animal data nor a significant interaction between pattern and paw (Figure 8B). Treatment with 6-OHDA evoked a significant worsening of forelimb akinesia as compared to intact animals specifically in the contralateral paw (Figure 8B). Additionally, the interaction between lesion state and paw was significant with post-hoc Tukey's tests demonstrating significant differences in contralateral paw performance between 6-OHDA treated and intact animals ($p = 0.0041$) and between contralateral and ipsilateral paw performance in 6-OHDA treated animals ($p = 0.0003$). Stimulation with regular 130Hz ameliorated the dysfunction of the contralateral paw in 6-OHDA treated animals (Figure 8B).

Forelimb use asymmetry test

No differences in forelimb akinesia as quantified by the cylinder test were detected with beta-patterned, continuous low frequency, or continuous high frequency stimulation in intact animals as compared to the no stimulation condition (**Table 6**, Figure 9), but these results are limited in a manner similar to those of the open field test. There was a significant effect of paw in both vertical exploration (Figure 9B) and landings (Figure 9C). Intact animals preferred bilateral forelimb use during vertical exploration to contralateral forelimb use ($p = 0.026$, Tukey's HSD), and this was unaffected by stimulation pattern. Similarly, when landing from a rear, intact animals preferred a balanced landing to ipsilateral forelimb ($p = 0.032$, Tukey's HSD) use across stimulation conditions. Interactions between pattern and paw were not significant for either vertical

682 exploration or landings. 6-OHDA treated animal performance did not differ significantly
683 from intact animal performance , and performance in 6-OHDA treated animals was not
684 improved with 130 Hz stimulation (Vertical exploration: Figure 9B; Landings: Figure 9C).
685 There was no effect of paw or a significant interaction term in either case. All lesions
686 were confirmed *in vivo* through use of the methamphetamine induced circling test.
687 However, intact animal baseline performance was limited (Figure 9B-C), and animals
688 lost interest in exploring the cylinder on repeated exposures. Thus, differences between
689 intact and 6-OHDA treated animal performance were difficult to detect.

690 ***Skilled forelimb reaching test***

691 No worsening of forelimb bradykinesia as assessed by the lever press was
692 detected with beta-patterned, continuous low frequency, or continuous high frequency
693 stimulation (**Table 7**, Figure 10). Stimulation in intact animals caused a statistically
694 significant worsening from intact baseline performance only for total trials attempted
695 (Figure 10B). Post-hoc Tukey's tests showed that patterns irregular beta ($p = 0.044$),
696 B20Hz IBF225Hz ($p = 0.035$), B25Hz IBF225Hz ($p = 0.021$), and regular 225Hz ($p =$
697 0.0025) all caused a decrease in total trials attempted from the no stimulation baseline
698 condition. However, given that the overall success rate at triggering pellet release and
699 quantitative metrics of lever push and release dynamics were unaffected by stimulation
700 pattern, this finding is likely not physiologically relevant. A statistically significant change
701 in mean press duration with stimulation in intact animals also was observed (Figure
702 10F), but post-hoc Tukey's testing found no significant differences among patterns
703 indicating that this finding also is likely not physiologically relevant.

704 The skilled forelimb reaching test did detect significant differences between
705 performance of intact and 6-OHDA treated animals (Table 7, Figure 10B-F). Treatment
706 with 6-OHDA caused a worsening of total trials attempted (Figure 10B); success rate
707 (Figure 10C); and minimum inter-press interval (Figure 10D). These results indicate that
708 6-OHDA lesioned rats attempted fewer trials, were less successful at triggering pellet
709 release when trials were attempted, and waited longer to initiate subsequent trials than
710 intact rats. Additionally, a near significant effect was found for initiation to hit peak
711 latency (Figure 10E) and mean press duration (Figure 10F). These results indicate that
712 6-OHDA lesioned rats trended towards an increase in time between the first and second
713 push in a given trial as indicated by the effect of lesion state on initiation to hit peak
714 latency. 6-OHDA lesioned rats also trended towards taking longer to release the lever
715 after each push as quantified by the mean press duration metric.

716 130 Hz stimulation applied to 6-OHDA lesioned rats improved the fraction of trials
717 that produced a pellet (Table 7, Figure 10C). Figure 10 also demonstrates a near
718 significant effect of 130 Hz stimulation on total trials attempted (Figure 10B) indicating a
719 trend towards an increase in total trials attempted when 130 Hz stimulation was applied.
720 Trends toward a rescue of performance on inter-press interval (Figure 10D), initiation to
721 hit peak latency (Figure 10E), and mean level press duration (Figure 10F) were seen
722 with 130 Hz stimulation. Additionally, the trends seen with 130 Hz stimulation were
723 similar to the improvements in 6-OHDA lesioned animal performance seen with
724 levodopa administration, which were less variable across rats and were statistically
725 significant (Figure 11). In particular, injection of levodopa increased total number of
726 trials attempted and success rate.

Effects of beta-patterned stimulation on behavior in 6-OHDA lesioned rats

We applied patterns of STN stimulation to 6-OHDA lesioned animals pre-treated with levodopa to control and increase BFP and assess whether the neural substrate changes inherent to the parkinsonian brain would amplify the effect of beta-patterned paradigms on motor function.

Adjusting steps test

Application of beta-patterned stimulation paradigms to levodopa-treated 6-OHDA-lesioned rats did not cause a detectable deterioration in motor performance in the paw contralateral to STN stimulation (Table 5, Figure 8). Additionally, there was no detectable effect of paw or an interaction of paw x stimulation pattern. Treatment with levodopa improved use of the contralateral paw in 6-OHDA treated rats (Figure 8C), but paw performance remained consistently high across beta-patterned, continuous low frequency, and continuous high frequency paradigms.

Skilled forelimb reaching test

Injection of levodopa significantly improved the total number of trials attempted (Figure 11A) and the rate of successful pellet release (Figure 11B), and there were trends toward decreasing the inter-trial interval (Figure 11C), the initiation to hit peak latency (Figure 11D), and the mean press duration (Table 7, Figure 11E). However, beta-patterned stimulation paradigms did not effect any detectable changes in performance metrics quantified by the lever press task as compared to levodopa-alone (Figure 11). The effect of stimulation patterns did not appear different from the effect of levodopa alone for the total number of trials (Figure 11A), success rate (Figure 11B), inter-trial interval (Figure 11C), initiation to hit peak latency (Figure 11D), and mean

press duration (Figure 11E) metrics. These data indicate that the stimulation patterns did not induce detectable symptoms of bradykinesia/akinesia in our levodopa-treated 6-OHDA-lesioned rat model.

Pre-6-OHDA single unit recordings

As beta-patterned stimulation did not cause a discernible worsening of motor performance in our behavioral tasks, we quantified SNr unit responses to STN stimulation to determine that we were indeed generating BFP with stimulation. The effect of STN stimulation on neural activity is displayed in Figure 12 for a representative SNr unit and summarized in Figure 13. STN stimulation caused changes in the ISI histograms from the pre-stimulation condition that mimicked the IPI histogram of the applied stimulation pattern. Figure 13A displays the fraction of total units assessed at each combination of stimulation pattern and amplitude. For a given pattern and amplitude, entrainment was defined as the presence of at least two consecutive bins in the normalized stimulation PSTH with counts above the $z = 4$ threshold. Entrainment fraction increased significantly with increasing amplitude (Table 8, Figure 13A). A significant effect of pattern and a significant interaction term were also found (Table 8, Figure 13A). Patterns generated equivocal degrees of entrainment with the exception of the continuous high frequency pattern, which was significantly worse at entraining units than beta-patterned or continuous low frequency paradigms ($p < 0.0001$ for all comparisons, Tukey's HSD; Figure 13B).

The average eEPF of entrained units as a function of stimulation pattern and amplitude is depicted in Figure 13C. Increasing stimulation amplitude caused a statistically significant increase in eEPF (Table 8, Figure 13C). The maximum eEPF values for each pattern ranged from 0.048 – 0.106 (Figure 13D), indicating that 4.8 to

10.6% of spikes recorded during stimulation were generated by the corresponding stimulation pattern. However, no statistically significant differences in average eEPF were found across patterns, nor was a significant interaction term found (Table 8, Figure 13C). For beta-patterned paradigms at the highest amplitudes, the latency of peak entrainment occurred in a range of 3-7.2 ms following a stimulus pulse. Additional smaller peaks at later times were also observed but were variable. For continuous low frequency stimulation at the highest amplitudes, two large peaks of entrainment occurred in latency ranges of 2.6-4.4 ms and 22.6-25.4 ms following a stimulus pulse. The continuous high frequency control had a peak of entrainment at a latency of 2.6-4.4 ms.

The difference in BFP of the SNr units between the baseline and stimulation conditions as a function of stimulation pattern and amplitude are displayed in Figure 13E. There was a significant effect of pattern (Table 8, Figure 13E) with a tendency toward burst-patterned paradigms causing greater increases in BFP in SNr units with stimulation as compared to the pre-stimulation baseline. In particular, post-hoc Tukey's testing showed that the B25Hz IBF225Hz pattern increased SNr unit BFP to a greater degree than the B15 IBF225Hz ($p = 0.04$), Regular 15Hz ($p < 0.0001$), Regular 20Hz ($p = 0.0004$), Regular 25Hz ($p = 0.02$), and Regular 225Hz ($p < 0.0001$) patterns (Figure 13F). The B20 IBF225Hz and Irregular beta patterns also increased SNr unit BFP to a greater degree than the Regular 15Hz (B20 IBF225Hz vs. Reg 15Hz: $p = 0.008$; Irregular Beta vs. Reg 15Hz: $p = 0.01$) and Regular 225Hz (B20 IBF225Hz vs. Reg 225Hz: $p < 0.0001$; Irregular Beta vs. Reg 225Hz: $p < 0.0001$) patterns (Figure 13F).

Finally, the B20 IBF 225Hz pattern increased SNr unit BFP to a greater degree than the Regular 20Hz ($p = 0.04$; Figure 13F).

Pre-6-OHDA electrocorticogram recordings

We quantified the effect of STN stimulation on ipsilateral M1 and contralateral S1 ECoG to determine whether stimulation was generating BFP at multiple points within the cortico-basal ganglia loop. The effect of STN stimulation on ECoG activity is displayed in Figure 14 for a representative animal and summarized in Figure 15. Figure 15A displays the difference in beta power fraction between ipsilateral M1 ECoG during stimulation and ipsilateral M1 ECoG before stimulation. The difference in beta power fraction increased with amplitude, and a significant effect of pattern and a significant interaction term were found (Table 9, Figure 15A). Most patterns generated equivalent amounts of BFP in ipsilateral M1 ECoG as compared to the pre-stimulation baseline. However, the B20 IBF225Hz pattern generated a significantly greater increase in BFP than Regular 20Hz continuous stimulation ($p = 0.04$, Tukey's HSD), and all patterns generated a significantly greater increase in BFP than the continuous high frequency pattern ($p < 0.05$), which did not generate an amount of BFP that was different from zero (Figure 15B).

Figure 15C displays the difference in beta power fraction between contralateral S1 ECoG during stimulation and contralateral S1 ECoG before stimulation. While there was a significant effect of amplitude, the increase in beta power fraction with stimulation was not significant (Table 9, Figure 15C).

The difference in BFP between ipsilateral M1 ECoG during stimulation and contralateral S1 ECoG during stimulation as a function of stimulation pattern and

amplitude is displayed in Figure 15E. The difference in beta power fraction increased significantly with amplitude (Table 9, Figure 15E). Also, as in SNr units, there was a significant effect of pattern with a significant interaction term (Table 9, Figure 15E). Post-hoc Tukey's test showed a tendency toward burst patterns causing greater increases in BFP in ipsilateral M1 ECoG vs contralateral S1 ECoG during stimulation. In particular, the B20 IBF 225Hz and the B25 IBF225Hz patterns increased BFP in ipsilateral M1 ECoG relative to contralateral S1 ECoG to a greater degree than the Regular 20Hz (B20 IBF 225Hz vs. Reg 20Hz: $p = 0.04$; B25 IBF225Hz vs. Reg 20Hz: $p = 0.02$) and Regular 225Hz (B20 IBF 225Hz vs. Reg 225Hz: $p = 0.0006$; B25 IBF225Hz vs. Reg 225Hz: $p = 0.0002$) patterns (Figure 15F). The B15 IBF225Hz and Irregular beta patterns also increased this difference in BFP to a greater degree than the Regular 225Hz (B15 IBF225Hz vs. Reg 225Hz: $p = 0.03$; Irregular Beta vs. Reg 225Hz: $p = 0.03$) pattern (Figure 15F). These data are consistent with the results of the computational model and the results of the SNr unit analysis, demonstrating that beta-patterned paradigms increase BFP at multiple sites in the cortico-basal ganglia circuit and do so more effectively than constant frequency stimulation.

Post-6-OHDA lesion single unit recordings

In 6-OHDA-lesioned rats not treated with levodopa, the effect of stimulation pattern and amplitude on fraction of units entrained, average eEPF, and change in beta power fraction was largely similar to that seen in intact animals (Figure 16). In 6-OHDA-lesioned animals not pre-treated with levodopa, significant effects of amplitude and pattern on entrainment fraction were found with no significant interaction term (Table 8, Figure 16A). Post-hoc Tukey's test found significant differences between B15 IBF225Hz and Regular 225Hz ($p = 0.02$) and B20 IBF225Hz and Regular 225Hz ($p = 0.04$; Figure

16B). Average eEPF was not affected by amplitude or pattern (Table 8, Figure 16C). Significant effects of amplitude and pattern were observed on the difference in beta power fraction in SNr units without a significant interaction term (Table 8, Figure 16E). Post-hoc Tukey's testing showed statistically significant differences between B25 IBF225Hz and patterns Regular 225Hz ($p < 0.0001$), Regular 15Hz ($p < 0.0001$), Regular 25Hz ($p = 0.0002$), Regular 20Hz ($p = 0.0002$), and B15 IBF 225Hz ($p = 0.02$; Figure 16F). Additional significant differences were found between Irregular Beta and patterns Regular 225Hz ($p < 0.0001$), Regular 15Hz ($p < 0.0001$), Regular 25Hz ($p = 0.0002$), and Regular 20Hz ($p = 0.0002$; Figure 16F). Finally, pattern B20 IBF225Hz was significantly different from Regular 225Hz ($p = 0.0023$) and Regular 15Hz ($p = 0.0062$), and pattern B15 IBF225Hz was significantly different from Regular 225Hz ($p = 0.0065$) and Regular 15Hz ($p = 0.02$; Figure 16F). Thus, overall, in 6-OHDA-lesioned animals not pre-treated with levodopa, entrainment fraction and average eEPF largely were equivocal across patterns (Figure 16B,D), but beta-patterned paradigms were superior to continuous low frequency paradigms at increasing SNr unit BFP, and continuous high frequency stimulation suppressed beta power (Figure 16F). Comparing across Figure 13 and Figure 16 using a multi-way ANOVA on factors amplitude, pattern, and lesion state, in addition to significant effects of amplitude and pattern, significant effects of lesion state on entrainment fraction ($p < 0.0001$, multi-way ANOVA, $F_{(1,0.40)} = 52.2$) and change in beta power fraction ($p < 0.0001$, multi-way ANOVA, $F_{(1,0.005)} = 21.6$) were found. No effect of lesion state on average eEPF was found ($p = 0.41$). Post-hoc student's t-test revealed that SNr units were more readily entrained in 6-OHDA lesioned animals ($p < 0.0001$) (Figure 13A-B vs. Figure 16A-B) but that more beta power was

induced in intact animals as compared to 6-OHDA lesioned animals ($p < 0.0001$) (Figure 13E-F vs. Figure 16E-F). The interpretation of these statistical differences between intact and 6-OHDA lesioned non-levodopa treated rats should be viewed with the caveat of a smaller sample of units analyzed in 6-OHDA lesioned animals than in intact animals.

Similar but weaker trends in SNr unit response to STN stimulation were seen in 6-OHDA lesioned animals treated with levodopa (Figure 16G-I). Entrainment fraction, average eEPF, and change in beta power fraction were compared across pattern and drug state in 6-OHDA lesioned rats. Statistically significant effects of drug state were found on entrainment fraction and beta power fraction, which both decreased in 6-OHDA lesioned rats in response to levodopa (Table 8, Figure 16G-I). A statistically significant effect of pattern was not found for entrainment fraction but was found for beta power fraction (Table 8, Figure 16G-I). However, post-hoc Tukey's test showed that beta-patterned paradigms remained superior to low frequency paradigms in amplifying beta power fraction in SNr units of 6-OHDA lesioned animals treated with levodopa. In particular, B25 IBF225Hz was significantly different from patterns Regular 20Hz ($p = 0.001$), Regular 15 Hz ($p = 0.0014$), Regular 25Hz (0.0027), and B15 IBF225Hz ($p = 0.02$; Figure 16I). Pattern irregular beta was significantly different from patterns Regular 20Hz ($p = 0.001$), Regular 15Hz ($p = 0.0014$), Regular 25Hz ($p = 0.0027$), and B15 IBF225Hz ($p = 0.022$; Figure 16I). Finally, pattern B20 IBF225Hz was significantly different from patterns Regular 20Hz ($p = 0.0064$), Regular 15Hz ($p = 0.01$), and Regular 25Hz ($p = 0.022$; Figure 16I).

DISCUSSION

A spectrum of data supports a correlation between beta frequency activity and bradykinesia and akinesia in PD, but evidence of causality is lacking. We investigated whether a causal link exists by applying novel patterns of stimulation that mimic the beta-frequency activity present in STN in PD to healthy animals to determine if they consequently exhibited parkinsonian symptoms. Single unit and ECoG recordings demonstrated that the patterns of STN stimulation entrained SNr unit activity and increased SNr unit and ipsilateral M1 ECoG BFP; beta-patterned stimulation paradigms were particularly effective. However, we did not detect changes in motor behavior with the applied stimulation across five validated measures of motor activity. The application of beta-ergic stimulation to 6-OHDA lesioned animals treated with levodopa to disrupt endogenous beta frequency activity similarly did not cause discernible changes in motor symptoms, suggesting that the parkinsonian neural substrate does not amplify the behavioral effects of induced beta activity introduced via the STN. Our results suggest that STN beta frequency oscillations (BFO) are not sufficient for the generation of bradykinetic/akinetic symptoms in PD.

Effect of beta-patterned stimulation on motor and neural activity in intact animals

Beta-ergic STN stimulation in healthy rats did not result in detectable worsening of motor performance metrics in our behavioral tasks. The skilled forelimb lever press test detected significant decreases from baseline in total trials attempted with some beta-patterned paradigms. However, the modest scale of these reductions and the lack of a corresponding decline of other performance metrics in this task suggests that this finding is not reflective of an induction of akinetic symptoms, particularly when

compared to the consequential reductions in performance resulting from 6-OHDA lesion. We used a battery of validated behavioral tests to quantify different metrics of forelimb and body bradykinesia. Three of five tasks–the bar test, adjusting steps test, and skilled forelimb lever press test–were sensitive to changes in performance after 6-OHDA lesion. Further, a minimum of five rats were used in these experiments, and given the effect sizes seen with 6-OHDA lesioning in Figure 6, Figure 8, and Figure 10, these behavioral tasks were powered to detect statistically significant differences between 6-OHDA and healthy rat performance with a power ≥ 0.80. The bar test and adjusting steps tests in particular were powered with n ≥ 5 rats (≥ 0.80) to detect effect sizes due to beta-ergic stimulation as small as 33% and 50% of the effect sizes caused by of 6-OHDA lesioning. Therefore, our study design was sufficiently powered to detected effect sizes that were meaningful and interesting for our hypothesis, and we acknowledge that more subtle deficits due to beta-ergic stimulation may have gone undetected. The open field test and forelimb use asymmetry tests did not detect changes in performance after 6-OHDA lesion. These tests are ‘passive’ rather than ‘active’ tasks and require that the animal is interested in exploring the test chamber, which is difficult to maintain over multiple trials. The 6-OHDA lesion state thus represented an important control in our behavioral studies, and these differences across tasks highlight the strength of our experimental design not relying on a single behavioral metric to assess our hypothesis.

As in the computational model, beta-patterned STN stimulation paradigms effectively entrained and increased beta frequency activity in SNr units and ipsilateral M1 ECoG in intact animals in a manner that increased with stimulation amplitude.

Regarding the effect on SNr unit activity, all beta-patterned and low frequency stimulation patterns equally entrained unit activity and did not differ significantly in average eEPF. These findings indicate that beta-patterned and low frequency stimulation captured and drove downstream neural activity equivalently. However, beta-patterned stimulation paradigms were superior to low frequency stimulation at inducing BFP. This finding supports our premise that bio-inspired stimulation patterns are better suited to driving beta frequency activity than low frequency stimulation patterns. Although eEPFs of 4.8-10.6% may seem small, these values align with those calculated by Agnesi et al. (8.7 ± 8.4%) for behaviorally effective high frequency STN DBS in MPTP treated rhesus monkeys, implying that the applied stimulation paradigms capture SNr unit activity in a manner similar to clinically effective DBS. Additionally, the observed latencies of peak entrainment for beta-patterned and low frequency stimulation paradigms were consistent with studies of excitatory post-synaptic current (EPSC) latencies between STN and SNr in rat brain slices. STN stimulation evoked complex EPSCs in the SNr consisting of an early monosynaptic current occurring at 4.6 ± 0.3 ms and variable, likely polysynaptic, later currents that were postulated to have been generated by stimulation of STN recurrent axon collaterals (Shen and Johnson, 2006). The latency at which the first peak of entrainment occurred for all patterns was consistent with the latency of this early monosynaptic current. The consistency of our results with these other studies supports the assertion that our beta-patterned STN stimulation paradigms were indeed generating beta frequency neural activity. One limitation of the eEPF calculation in assessing SNr unit entrainment to stimulation is that shorter IPIs reduce the probability of detecting a spike within that window. The Regular

225Hz pattern performed worse at entraining SNr units according to this metric as the IPI comprised 4.4 ms. When this pattern did entrain units, it generated spikes in a manner comparable to that of the other patterns and effectively suppressed BFP as predicted by the computational model.

The beta-ergic patterns of STN stimulation used in the present study were delivered continuously and without reference to the phase of the endogenous beta activity. Cagnan et al. demonstrated that DBS of the thalamus produced differential effects on tremor in patients with essential tremor, dependent upon the phase of the tremor cycle when the (burst of) stimulation was delivered (Cagnan et al., 2017). However, the relationship between the stimulation bursts and the phase of tremor wandered during continuous stimulation, and the phase of tremor when any particular burst of stimulation was delivered was variable. Therefore, given the comparatively long epochs of stimulation that we employed, we expect that the bursts of beta-ergic stimulation wandered across the entire range of phase of any intrinsic beta activity. As our in vivo recordings demonstrated induction of substantial beta-bad oscillatory activity, we do not expect that phase-dependent stimulation would yield results different than those reported here.

Similar effects were seen on the ECoG activity. Stimulation patterns significantly increased beta power fraction in ipsilateral M1 ECoG as compared to the pre-stimulation baseline. However, the B20 IBF225Hz pattern was superior in generation of BFP than its corresponding low frequency control pattern. Contralateral S1 ECoG served as a control. While ipsilateral projections between S1 and STN have been seen in a rat histological study, no evidence of a connection between contralateral S1 and

STN was found (Canteras et al., 1988). Comparing the results in ipsilateral M1 and contralateral S1 provides a sense of how much BFP in the calculated spectra is due to the lingering effects of stimulation artifact after data processing (contralateral S1) versus a true physiological effect of stimulation (ipsilateral M1). The effects of stimulation on BFP in contralateral S1 ECoG were not significantly different across pattern and not much different from zero. Relating ipsilateral M1 ECoG spectral power results to contralateral S1 spectral power results during stimulation further enhanced the difference seen across patterns with B20 IBF225Hz and B25 IBF225Hz patterns demonstrating a significantly greater increase in BFP than the low frequency Regular 20Hz pattern. These results, in combination with the lack of bradykinetic/akinetic symptom generation in any motor task, further indicate a lack of a causal relationship between STN BFO and bradykinesia/akinesia in PD.

Effect of beta-patterned stimulation on motor and neural activity in 6-OHDA lesioned animals

As in intact animals, performance in the adjusting steps and skilled forelimb reaching tests were unaffected in a discernable manner by beta-patterned STN stimulation in levodopa-treated 6-OHDA lesioned rats. In both tasks, 130Hz stimulation and injection of levodopa significantly improved motor performance highlighting the sensitivity of the task to changes in bradykinetic/akinetic symptoms. The animals, however, continued to perform at a high level with beta-patterned STN stimulation.

In 6-OHDA lesioned rats not treated with levodopa, beta-patterned STN stimulation paradigms were largely as effective at entraining and increasing beta frequency activity in SNr units as in intact rats. Similarly, while all beta-patterned and

low frequency stimulation patterns equally entrained unit activity and did not differ in average eEPF, beta-patterned stimulation was superior to low frequency controls in increasing beta frequency activity in SNr units in untreated 6-OHDA lesioned animals. Injection of levodopa weakened stimulation-induced unit entrainment and induction of BFP. Levodopa reduces beta band synchrony in PD patients and 6-OHDA lesioned rats (Levy et al., 2002). A potential limitation of our study design is that rather than simply disrupting endogenous beta oscillatory activity, the effects of levodopa may have counteracted the ability to induce artificial synchrony as strongly as in intact and non-levodopa treated 6-OHDA lesioned animals. Furthermore, the same lesioned animal cohort participated in SNr unit recordings with and without levodopa treatment; channel waveform comparisons confirmed that the units analyzed in both lesion studies were largely identical (data not shown). These observations suggest that a true biological effect lay behind the effect of drug state in the comparative analysis of entrainment of SNr unit activity in 6-OHDA lesioned animals with and without levodopa treatment. Our goal in applying the same methodology to intact animals and to levodopa-treated 6-OHDA lesioned animals was to see if the inherent changes in neural circuitry in PD would amplify or unmask the effect of our beta-ergic patterns. However, induction of BFP in SNr unit activity in 6-OHDA lesioned animals not treated with levodopa did not exceed –and was slightly less than– that seen in intact animals.

In summary, we did not detect a causal link between STN beta frequency activity and bradykinesia/akinesia in PD within the limits of our experimental design. Other studies have pursued a similar objective but focused on introducing continuous low frequency STN stimulation at beta band frequencies in intact or PD subjects and

assessing potential deleterious effects on motor performance (Chen et al., 2007; Pogosyan et al., 2009, Syed et al., 2012). We designed unique bursting patterns of stimulation intended to mimic the activity seen in STN cells in PD to amplify beta frequency activity, and applied them, along with continuous low frequency stimulation, to the STN of intact and 6-OHDA lesioned rats. We confirmed that our patterns entrained neural activity in downstream nuclei *in vivo* as compared to other studies that demonstrate this phenomenon *in vitro* (Syed et al., 2012) and confirmed entrainment of neural activity in the same animals that performed the motor tasks. While low frequency stimulation and the novel bursting patterns equally entrained SNr units, the novel bursting patterns were superior at amplifying beta frequency activity as compared to the low frequency stimulation used in prior studies. Yet, we detected no impact on motor performance despite use of an extensive battery of behavioral tasks to assess forelimb bradykinesia/akinesia that were sensitive enough to detect deterioration in motor performance following 6-OHDA lesioning with a minimum of three rats. We do not claim to have proven that a link between STN beta frequency activity and bradykinesia/akinesia in PD does not exist. Indeed, such a claim cannot be proved, and we acknowledge several limitations of our study. The artificial beta band power we generated may be fundamentally different from the broad band endogenous beta power that emerges across neural circuits in 6-OHDA rats and patients with PD. Additionally, it is unclear from studies of parkinsonian models and PD patients what magnitude of BFP would be expected to correlate with a debilitating degree of bradykinesia for which the subject could not compensate. Finally, while we assessed motor performance in a variety of tasks, the majority of these tasks measure gross body or limb

bradykinesia/akinesia, and different behavioral tasks aimed at quantifying more subtle metrics of limb bradykinesia may have yielded evidence of induced deficits.

Given these limitations, while our approach was novel, our results do concur with those of other groups that found no (Syed et al., 2012) or slight (Chen et al., 2007; Pogosyan et al., 2009) effects on motor performance of imposed STN beta frequency activity in pre-clinical and clinical studies. Our results complement the existing body of work exploring the relationship of STN beta frequency activity and bradykinesia/akinesia in PD, which call into question this assumed correlative link between BFO and bradykinesia in PD. Elucidating the pathophysiology of PD motor symptoms and the origin of BFO will impact the understanding of the field and the effectiveness of treatment options.

REFERENCES

Agnesi F, Muralidharan A, Baker KB, Vitek JL, Johnson MD (2015) Fidelity of frequency and phase entrainment of circuit-level spike activity during DBS. J Neurophysiol 114:825-834.

Alves G, Forsaa EB, Pedersen KF, Gjerstad MD, Larsen JP (2008) Epidemiology of Parkinson's disease. J Neurol 255:18-32.

Birdno MJ, Grill WM (2008) Mechanisms of deep brain stimulation in movement disorders as revealed by changes in stimulus frequency. Neurotherapeutics 5:14-25.

Blanca MJ, Alarcón R, Arnau J, Bono R, Bendayan R (2017) Non-normal data: Is ANOVA still a valid option? Psicothema 29:552-557.

Brocker DT, Swan BD, So RQ, Turner DA, Gross RE, Grill WM (2017) Optimized temporal pattern of brain stimulation designed by computational evolution. Sci Transl Med 9:1-11.

Bronte-Stewart H, Barberini C, Koop MM, Hill BC, Henderson JM, Wingeier B (2009) The STN beta-band profile in Parkinson's disease is stationary and shows prolonged attenuation after deep brain stimulation. Exp Neurol 215:20-28.

Brown P, Oliviero A, Mazzone P, Insola A, Tonali P, Lazzaro VD (2001) Dopamine dependency of oscillations between subthalamic nucleus and pallidum in Parkinson's disease. J Neurosci 21:1033-1038.

Cagnan H, Pedrosa D, Little S, Pogosyan A, Cheeran B, Aziz TZ, Green AL, Fitzgerald J, Foltynie T, Limousin P, Zrinzo L, Hariz M, Friston KJ, Denison T, Brown P (2017) Stimulating at the right time: phase-specific deep brain stimulation. Brain 140:132-145.

1083 Canteras NS, Shammah-Lagnado SJ, Silva BA, Ricardo JA (1988) Somatosensory
1084 inputs to the subthalamic nucleus: a combined retrograde and anterograde horseradish
1085 peroxidase study in the rat. Brain Res 458:53-64.
1086 Carvalho MM, Campos FL, Coimbra B, Pedo JM, Rodrigues C, Lima R, Rodrigues AJ,
1087 Sousa N, Salgado AJ (2013) Behavioral characterization of the 6-hydroxidopamine
1088 model of Parkinson's disease and pharmacological rescuing of non-motor deficits. Mol
1089 Neurodegener 8:14.
1090 Chang J-W, Wachtel SR, Young D, Kang U-J (1999) Biochemical and anatomical
1091 characterization of forepaw adjusting steps in rat models of Parkinson's disease: studies
1092 on medial forebrain bundle and striatal lesions. Neuroscience 88:617-628.
1093 Chen CC, Litvak V, Gilbertson T, Kuhn A, Lu CS, Lee ST, Tsai CH, Tisch S, Limousin
1094 P, Hariz M, Brown P (2007) Excessive synchronization of basal ganglia neurons at
1095 20Hz slows movement in Parkinson's disease. Exp Neurol 205:214-221.
1096 Connor B, Kozlowski D, Schallert T, Tillerson J, Davidson B, Bohn M (1999) Differential
1097 effects of glial cell line-derived neurotrophic factor (GDNF) in the striatum and
1098 substantia nigra of the aged Parkinsonian rat. Gene Ther 6:1936-1951.
1099 Dauer W, Przedborski S (2003) Parkinson's disease: mechanisms and models. Neuron
1100 39:889-909.
1101 Degos B, Deniau J-M, Chavez M, Muarice N (2009) Chronic but not acute dopaminergic
1102 transmission interruption promotes a progressive increase in cortical beta frequency
1103 synchronization: relationships to vigilance state and akinesia. Cereb Cortex 19:1616-
1104 1630.

1105 Delaville C, McCoy AJ, Gerber CM, Cruz AV, Walters JR (2015) Subthalamic nucleus
1106 activity in the awake hemiparkinsonian rat: relationships with motor and cognitive
1107 networks. J Neurosci 35:6918-6930.
1108 Dorval AD, Kuncel AM, Birdno MJ, Turner DA, Grill WM (2010) Deep brain stimulation
1109 alleviates parkinsonian bradykinesia by regularizing pallidal activity. J Neurophysiol
1110 104:911-921.
1111 Duty S, Jenner P (2011) Animal models of Parkinson's disease: a source of novel
1112 treatments and clues to the cause of the disease. Br J Pharmacol 164:1357-1391.
1113 Eusebio A, Brown P (2009) Synchronisation in the beta frequency-band - The bad boy
1114 of parkinsonism or an innocent bystander? Exp Neurol 217:1-3.
1115 Fang X, Sugiyama K, Akamine S, Namba H (2006) Improvements in motor behavioral
1116 tests during deep brain stimulation of the subthalamic nucleus in rats with different
1117 degrees of unilateral parkinsonism. Brain Res 1120:202-210.
1118 Fleming SM (2009) Behavioral outcome measures for the assessment of sensorimotor
1119 function in animal models of movement disorders. Int Rev Neurobiol 89:57-65.
1120 Gale JT, Shields DC, Jain FA, Amirnovin R, Eskandar EN (2009) Subthalamic nucleus
1121 discharge patterns during movement in the normal monkey and Parkinsonian patient.
1122 Brain Res 1260:15-23.
1123 Gatev P, Darbin O, Wichmann T (2006) Oscillations in the basal ganglia under normal
1124 conditions and in movement disorders. Mov Disord 21:1566-1577.
1125 Glajch KE, Fleming SM, Surmeier DJ, Osten P (2012) Sensorimotor assessment of the
1126 unilateral 6-hydroxydopamine mouse model of Parkinson's disease. Behav Brain Res
1127 230:309-316.

1128 Hays SA, Khodaparast N, Sloan AM, Fayyaz T, Hulsey DR, Ruiz AD, Pantoja M, Kilgard
1129 MP, II RLR (2013) The bradykinesia assessment task: an automated method to
1130 measure forelimb speed in rodents. J Neurosci Methods 214:52-61.
1131 Holtbernd F, Eidelberg D (2012) Functional brain networks in movement disorders:
1132 recent advances. Curr Opin Neurol 25:392-401.
1133 Kuhn AA, Trottenberg T, Kivi A, Kupsch A, Schneider G-H, Brown P (2005) The
1134 relationship between local field potential and neuronal discharge in the subthalamic
1135 nucleus of patients with Parkinson's disease. Exp Neurol 194:212-220.
1136 Kuhn AA, Kupsch A, Schneider G-H, Brown P (2006) Reduction in subthalamic 8-35 Hz
1137 oscillatory activity correlates with clinical improvement in Parkinson's disease. Eur J
1138 Neurosci 23:1956-1960.
1139 Kuhn AA, Kempf F, Brucke C, Doyle LG, Martinez-Torres I, Pogosyan A, Trottenberg T,
1140 Kupsch A, Schneider G-H, Hariz MI, Vandenberghe W, Nuttin B, Brown P (2008) High-
1141 frequncy stimulation of the subthalamic nucleus suppresses oscillatory beta activity in
1142 patients with Parkinson's disease in parallel with improvement in motor performance. J
1143 Neurosci 28:6165-6173.
1144 Kumaravelu K, Brocker DT, Grill WM (2016) A biophysical model of the cortex-basal
1145 ganglia-thalamus network in the 6-OHDA lesioned rat model of Parkinson's disease. J
1146 Comput Neurosci 40:207-229.
1147 Levy R, Hutchison WD, Lozano AM, Dostrovsky JO (2000) High-frequency
1148 synchronization of neuronal activity in the subthalamic nucleus of parkinsonian patients
1149 with limb tremor. J Neurosci 20:7766-7775.

1150 Levy R, Ashby P, Hutchison WD, Lang AE, Lozano AM, Dostrovsky JO (2002)
1151 Dependence of subthalamic nucleus oscillations on movement and dopamine in
1152 Parkinson's disease. Brain 125:1196-1209.
1153 Mallet N, Pogosyan A, Sharott A, Csicsvari J, Bolam JP, Brown P, Magill PJ (2008)
1154 Disrupted dopamine transmission and the emergence of exaggerated beta oscillations
1155 in subthalamic nucleus and cerebral cortex. J Neurosci 28:4795-4806.
1156 McCarthy MM, Moore-Kochlacs C, Gu X, Boyden ES, Han X, Kopell N (2011) Striatal
1157 origin of the pathologic beta oscillations in Parkinson's disease. PNAS 108:11620-
1158 11625.
1159 McConnell GC, So RQ, Hilliard JD, Lopomo P, Grill WM (2012) Effective deep brain
1160 stimulation suppresses low-frequency network oscillations in the basal ganglia by
1161 regularizing neural firing patterns. J Neurosci 32:15657-15668.
1162 Moran A, Stein E, Tischler H, Bar-Gad I (2012) Decoupling neuronal oscillations during
1163 subthalamic nucleus stimulation in the parkinsonian primate. Neurobiol Dis 45:583-590.
1164 Normal G (2010) Likert scales, levels of measurement and the “laws” of statistics.
1165 Advances in Health Sciences Education 15:625-632.
1166 Paxinos G, Watson C, The Rat Brain in Stereotaxic Coordinates, Fifth ed., Elsevier
1167 Academic Press, Burlington, MA, 2005.
1168 Pearson E (1931) The Analysis of Variance in Cases of Non-Normal Variation.
1169 Biometrika 23:114-133.
1170 Plenz D, Kital ST (1999) A basal ganglia pacemaker formed by the subthalamic nucleus
1171 and external globus pallidus. Nature 400:677-682.

1172 Pogosyan A, Gaynor LD, Eusebio A, Brown P (2009) Boosting cortical activity at beta-
1173 band frequencies slows movement in humans. Curr Biol 19:1637-1641.
1174 Putterman DB, Munhall AC, Kozell LB, Belknap JK, Johnson SW (2007) Evaluation of
1175 levodopa dose and magnitude of dopamine depletion as risk factor for levodopa-
1176 induced dyskinesia in a rat model of Parkinson's disease. J Pharmacol Exp Ther
1177 323:277-284.
1178 Schallert T, Fleming SM, Leasure JL, Tillerson JL, Bland ST (2000) CNS plasticity and
1179 assessment of forelimb sensorimotor outcome in unilateral rat models of stroke, cortical
1180 ablation, parkinsonism and spinal cord injury. Neuropharmacology 39:777-787.
1181 Sharott A, Magill PJ, Harnack D, Kupsch A, Meissner W, Brown P (2005) Dopamine
1182 depletion increases the power and coherence of beta-oscillations in the cerebral cortex
1183 and subthalamic nucleus of the awake rat. Eur J Neurosci 21:1413-1422.
1184 Shen K-Z, Johnson SW (2006) Subthalamic stimulation evokes complex EPSCs in the
1185 rat substantia nigra pars reticulata in vitro. J Physiol 573:697-709.
1186 So RQ, McConnell GC, August AT, Grill WM (2012) Characterizing effects of
1187 subthalamic nucleus deep brain stimulation on methamphetamine-induced circling
1188 behavior in hemi-parkinsonian rats. IEEE Trans Neural Syst Rehabil Eng 20:626-635.
1189 Stein E, Bar-Gad I (2013) Beta oscillations in the cortico-basal ganglia loop during
1190 parkinsonism. Exp Neurol 245:52-59.
1191 Syed ECJ, Benazzouz A, Taillade M, Baufreton J, Champeaux K, Falgairolle M, Bioulac
1192 B, Gross CE, Boraud T (2012) Oscillatory entrainment of subthalamic nucleus neurons
1193 and behavioural consequences in rodents and primates. Eur J Neurosci 36:3246-3257.

1194 Tieu K (2011) A guide to neurotoxic animal models of Parkinson's disease. Cold Spring
1195 Harb Perspect Med 1:a009316.
1196 Ungerstedt U, Arbuthnott GW (1970) Quantitative recording of rotational behavior in rats
1197 after 6-hydroxy-dopamine lesions of the nigrostriatal dopamine system. Brain Res
1198 24:485-493.
1199 Welter M-L, Burbaud P, Fernandez-Vidal S, Bardinet E, Coste J, Piallat B, Borg M,
1200 Besnard S, Sauleau P, Devaux B, Pidoux B, Chaynes P, Montcel STd, Bastian A,
1201 Langbour N, Teillant A, Haynes W, Yelnik J, Karachi C, Mallet L (2011) Basal ganglia
1202 dysfunction in OCD: subthalamic neuronal activity correlates with symptoms severity
1203 and predicts high-frequency stimulation efficacy. Transl Psychiatry 1:e5.
1204 Yamawaki N, Stanford IM, Hall SD, Woodhall GL (2008) Pharmacologically induced and
1205 stimulus evoked rhythmic neuronal oscillatory activity in the primary motor cortex in
1206 vitro. J Neurosci 151:386-395.
1207

ILLUSTRATIONS AND TABLES

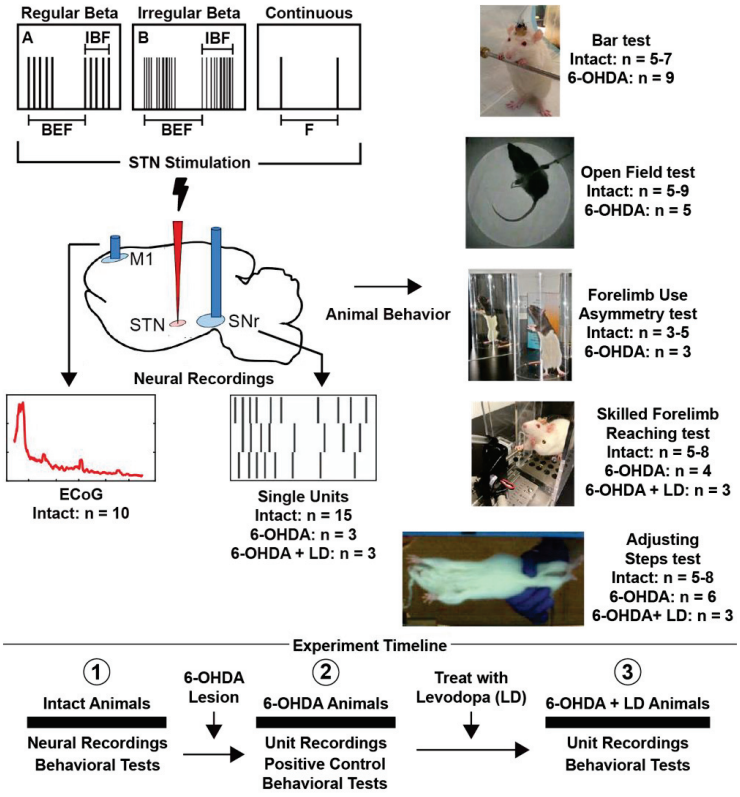

Figure 1. Experimental design to assess the effects of beta-ergic deep brain stimulation on neural activity and motor function. 1) Different temporal patterns of STN stimulation were applied in random order to intact rats. The effects on downstream SNr single units and M1 ECoG were recorded to quantify induced beta. Rats performed a variety of behavioral tasks during beta-ergic stimulation to assess impact of stimulation oon bradykinesia/akinesia. 2) Rats were then unilaterally lesioned via injection of 6-OHDA into the medial forebrain bundle. Beta-ergic stimulation patterns were again applied in random order, and the effect on SNr single units was recorded. The performance of 6-OHDA lesioned rats was assessed in all behavioral tasks with and without 130Hz stimulation. 3) Finally, 6-OHDA lesioned rats were treated with levodopa, and the effect of beta-ergic stimulation patterns on SNr units was recorded. The performance of levodopa-treated 6-OHDA rats in the adjusting steps and skilled forelimb reaching task was quantified

during different patterns of beta-ergic stimulation. IBF = Intra-Burst Frequency. BEF = Burst Envelope Frequency. LD = Levodopa.

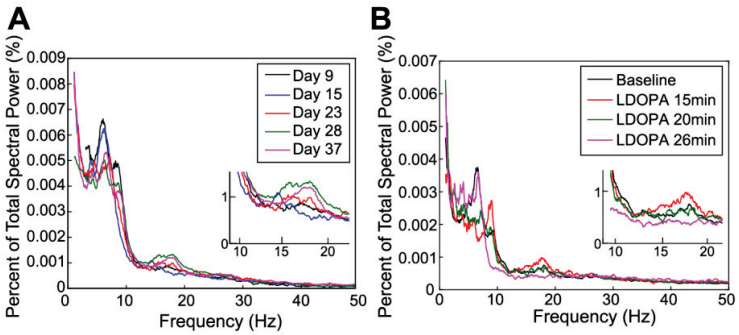

Figure 2. Sample post-6-OHDA lesion ipsilateral M1 ECoG recordings. Insets show a magnified view of beta frequency range results. **A:** Progressive increase in ipsilateral M1 beta frequency activity as a function of days post-6-OHDA lesion. **B:** Disruption of ipsilateral M1 beta frequency activity as a function of time from injection of levodopa (LDOPA).

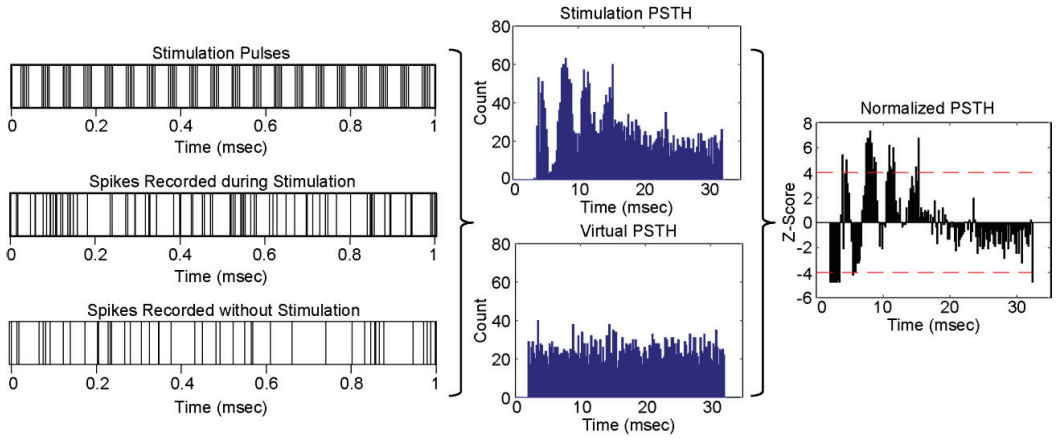

Figure 3. Calculation of normalized post-stimulus time histogram (PSTH). Artifact timestamps were used to create a PSTH for the stimulation period and a 'virtual' PSTH for the pre-stimulation period. Bin counts for the stimulation PSTH were converted to z-scores using the virtual PSTH bin counts to determine statistically significant changes in activity due to applied STN stimulation.

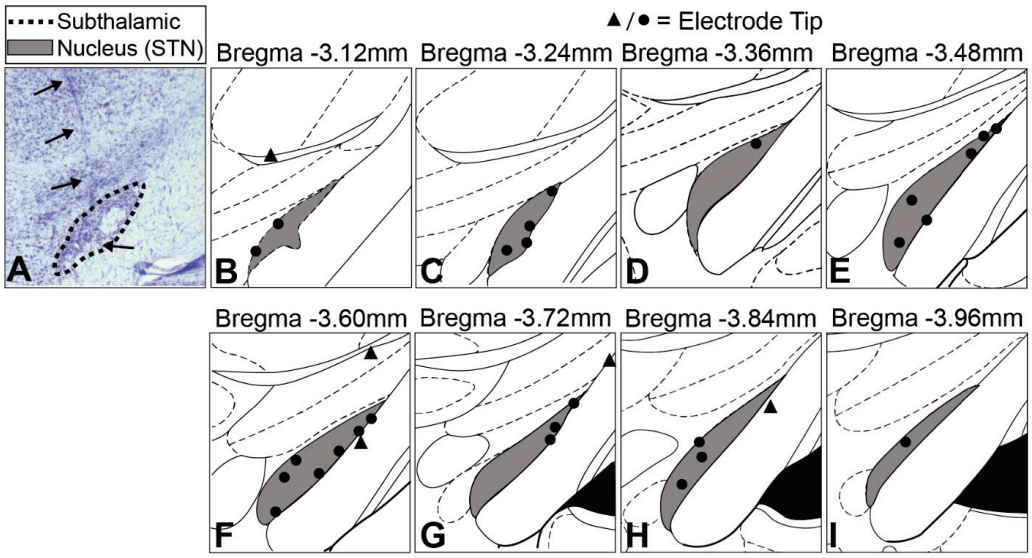

Figure 4. Histological analysis of STN electrode positions. **A**: Light microscopy image of cresyl violet stained brain slice. Dashed line denotes outline of STN. Arrows indicate electrode track. **B-I**: Locations of STN electrode tips. Each circle (●) or triangle (▲) indicates the location of the deepest electrode tip for one animal. Only animals with electrode tips in the STN (●) were included in analysis. Animals with electrode tips outside of the STN (▲) were excluded from analysis.

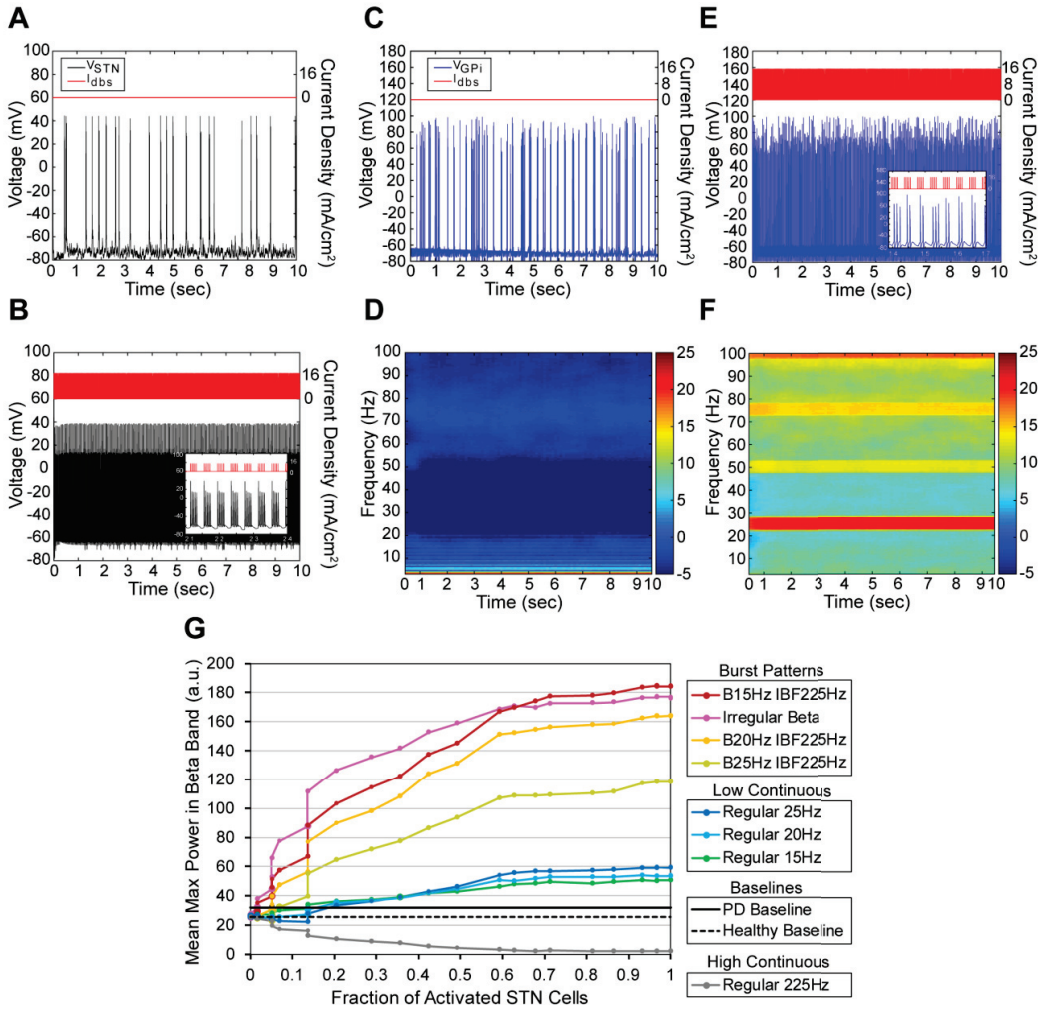

Figure 5. Effect of stimulation patterns on neuronal activity in a biophysically-based computational model of the basal ganglia. **A**: Model STN neuron voltage output with no applied STN input. **B**: Model STN neuron voltage output with pattern B25 IBF225 applied to STN and 100% STN cell activation (n = 59 cells). **C**: Model GPi neuron voltage output with no applied STN input. **D**: Averaged spectrogram of GPi neuron voltage output with no applied STN input (n = 59 cells). **E**: Model GPi neuron voltage output with pattern B25 IBF225 applied to STN and 100% STN neuron activation. Inset: Burst activity in GPi neuron in response to burst patterned STN input. **F**: Averaged spectrogram of GPi neuron voltage output with pattern B25 IBF225 applied to STN and 100% STN neuron activation (n = 59 cells). **G**: Mean maximum

power in the beta band as a function of fraction of STN neurons activated and stimulation pattern. Dashed black line ('Healthy Baseline') and solid black line ('PD Baseline') indicate baseline GPi beta band power with no applied STN stimulation when model is run in either healthy or parkinsonian states, respectively. Two-way ANOVA performed on log-transformed data revealed a significant effect of pattern ($p < 0.0001$), log(fraction of activated STN cells) ($p < 0.0001$), and a significant interaction term ($p < 0.0001$). Post-hoc Tukey's test found a significant difference between the increase in log(mean max beta) caused by each bursting pattern–both regular and irregular–in the model as compared to the increase caused by each continuous low frequency patterns ($p < 0.0001$ for all comparisons). Additionally, post-hoc Tukey's test found a significant difference between Regular 225 Hz and Healthy Baseline ($p < 0.0001$) and between Regular 225 Hz and PD Baseline ($p < 0.0001$). Error bars indicate mean ± SD (n = 10 simulations).

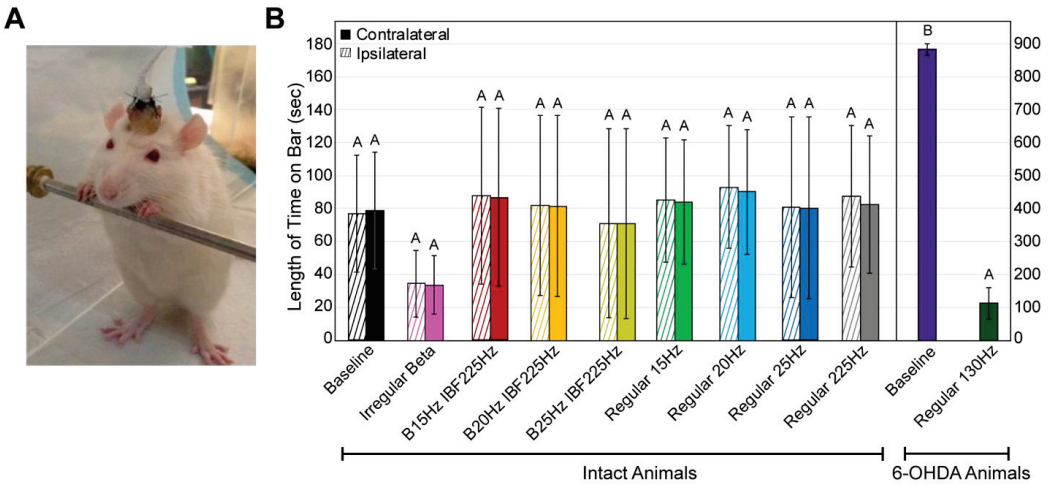

Figure 6. Effect of STN stimulation patterns on performance in bar test. 'Contralateral' refers to the side of the body contralateral to the brain hemisphere to which stimulation was applied. Error bars indicate mean ± SE. Patterns not sharing the same letter are significantly different from each other ($p < 0.05$). **A**: Rat was placed in an upright position with its forepaws resting on a bar 10 cm above the ground. **B**: Length of time on bar as a function of stimulation pattern, lesion state, and forepaw. Two-way repeated measures ANOVA performed on healthy (intact) animal data was not significant in length of time on bar for pattern ($p = 0.92$), paw ($p = 0.34$), or pattern x paw ($p = 0.74$). See **Table 1** for *n* for each pattern. A statistically significant difference in length of time on bar between baseline 6-OHDA treated animal ($n = 9$) contralateral paw performance and intact animal ($n = 7$) baseline contralateral paw performance was found ($p < 0.0001$, Wilcoxon rank sum test). A statistically significant difference in length of time on bar between baseline 6-OHDA treated animal performance ($n = 9$) performance and performance of 6-OHDA treated animals with 130 Hz stimulation was found ($p < 0.0001$, Wilcoxon rank sum test).

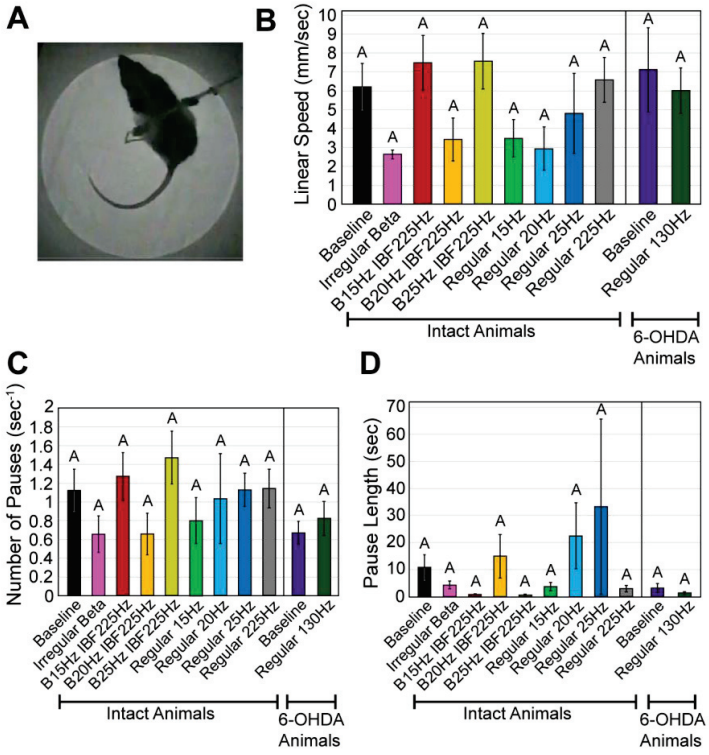

Figure 7. Effect of STN stimulation patterns on performance in open field test. Error bars indicate mean ± SE. Patterns not sharing the same letter are significantly different from each other ($p < 0.05$). **A**: Rat was placed in a dark cylindrical chamber and its movements were video-recorded. **B**: Linear speed as a function of stimulation pattern and lesion state. One-way repeated measures ANOVA performed on intact animal data found no significant effect of pattern ($p = 0.15$). See **Table 1** for *n* for each pattern. An unpaired t-test performed on 6-OHDA treated animal ($n = 5$) baseline performance vs. intact animal ($n = 9$) baseline performance found no significant effect of lesion state ($p = 0.72$). A paired t-test performed on 6-OHDA treated animal data ($n = 5$) found no significant effect of 130Hz stimulation ($p = 0.54$). **C**: Number of pauses per second as a function of stimulation pattern and lesion state. One-way repeated measures ANOVA performed on intact animal data found no significant effect of pattern ($p = 0.16$). See **Table 1** for *n* for each pattern. An unpaired t-test performed on 6-OHDA treated animal ($n = 5$) baseline performance vs. intact animal ($n = 9$) baseline performance found no significant effect of lesion state ($p = 0.11$). A paired t-test performed on 6-OHDA treated animal data ($n = 5$) found no significant effect of 130Hz

stimulation (p = 0.22). **D**: Pause length as a function of stimulation pattern and lesion state. One-way repeated measures ANOVA performed on intact animal data found no significant effect of pattern (p = 0.44). See **Table 1** for *n* for each pattern. An unpaired t-test performed on 6-OHDA treated animal (*n* = 5) baseline performance vs. intact animal (*n* = 9) baseline performance found no significant effect of lesion state (p = 0.17). A paired t-test performed on 6-OHDA treated animal data (*n* = 5) found no significant effect of 130Hz stimulation (p = 0.30).

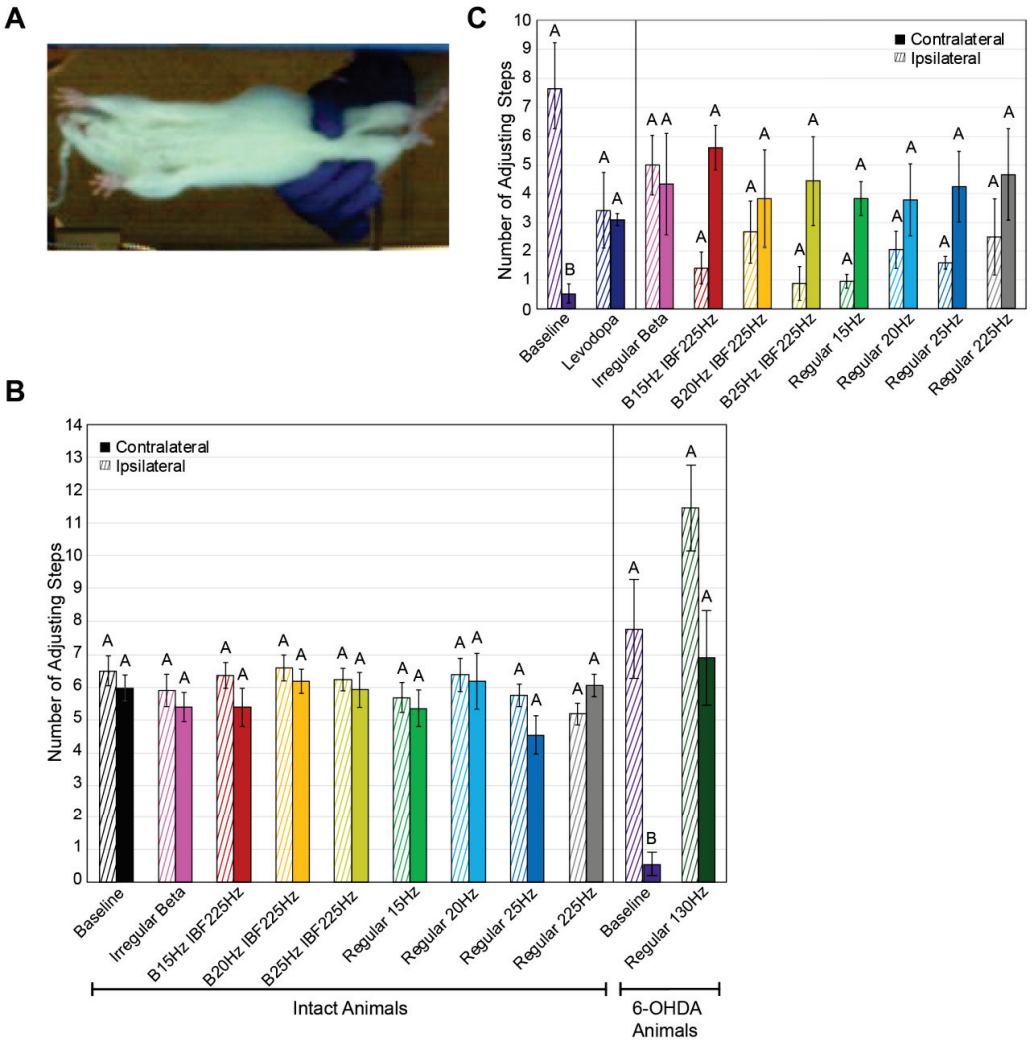

Figure 8. Effect of STN stimulation patterns on performance in adjusting steps test. 'Contralateral' refers to the side of the body contralateral to the brain hemisphere to which stimulation was applied. Error bars indicate mean ± SE. Patterns not sharing the same letter are significantly different from each other ($p < 0.05$). **A**: The rat was suspended such that its forepaws bore its weight as it was dragged backwards along a clear glass surface. Adjusting steps were video-recorded from below. **B**: Number of forepaw adjusting steps made as a function of stimulation pattern, lesion state, and forepaw. Two-way repeated measures ANOVA performed on intact animal data was not significant for pattern ($p = 0.48$), paw ($p =$

0.28), or pattern x paw (p = 0.10). See **Table 1** for *n* for each pattern. Two-way repeated measures ANOVA performed between intact animal data (*n* = 8) and baseline 6-OHDA treated animal data (*n* = 6) found significant effects of lesion state (p = 0.0498), paw (p = 0.039), and lesion state x paw (p = 0.0007). Post-hoc Tukey's test on lesion state x paw interaction found significant differences between 6-OHDA treated and intact animal contralateral paw performance (p = 0.0041) and between 6-OHDA treated animal contralateral and ipsilateral paw performance (p = 0.0003). Two-way repeated measures ANOVA performed on 6-OHDA treated animal data found a significant effect of pattern (p = 0.019), a significant effect of paw (p = 0.024), but no significant interaction term. **C:** Number of forepaw adjusting steps made by levodopa-treated 6-OHDA rats as a function of stimulation pattern, drug state, and forepaw. An unpaired t-test performed on contralateral paw performance with (*n* = 3) and without (*n* = 6) levodopa and without applied stimulation found a significant effect of drug state (p = 0.0001). Two-way repeated measures ANOVA performed on levodopa-treated 6-OHDA rats was not significant for pattern (p = 0.31), paw (p = 0.10), or pattern x paw (p = 0.13). See **Table 1** for *n* for each pattern.

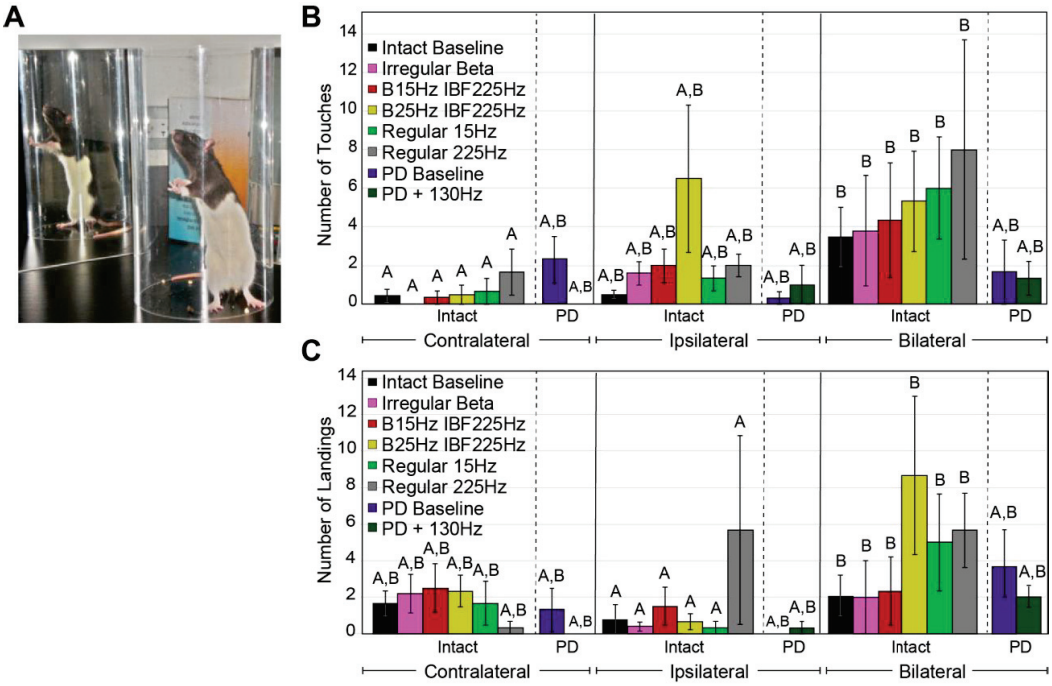

Figure 9. Effect of STN stimulation patterns on performance in the forelimb use asymmetry test. 'Contralateral' refers to the side of the body contralateral to the brain hemisphere to which stimulation was applied. Error bars indicate mean ± SE. Patterns not sharing the same letter are significantly different from each other ($p < 0.05$). **A**: Rat was placed in a clear cylinder and vertical exploration of the cylinder was video recorded. **B**: Preferred forelimb use in vertical exploration as a function of stimulation pattern and lesion state. Two-way repeated measures ANOVA performed on intact animal data revealed a significant effect of paw ($p = 0.026$), but no significant effect of pattern ($p = 0.55$) or pattern x paw ($p = 0.72$). See **Table 1** for *n* for each pattern. Post-hoc Tukey's test on factor paw found bilateral touches during vertical exploration to be significantly greater than contralateral paw touches across all stimulation patterns in intact animals ($n = 8$, $p = 0.021$). Two-way repeated measures ANOVA performed on intact ($n = 8$) vs. 6-OHDA treated ($n = 3$) animal baseline performance found no significant effect of paw ($p = 0.10$), lesion state ($p = 0.98$), or paw x lesion state ($p = 0.34$). Two-way repeated measures ANOVA performed on 6-OHDA treated ($n = 3$) animal data found no significant effect of paw ($p = 0.53$), pattern ($p = 0.42$), or paw x pattern ($p = 0.44$) with 130Hz stimulation. **C**: Preferred forelimb use in landing as a

function of stimulation pattern and lesion state. Two-way repeated measures ANOVA performed on intact animal data found a significant effect of paw ($p = 0.021$), but no significant effect of pattern ($p = 0.36$) or pattern x paw ($p = 0.32$). See **Table 1** for *n* for each pattern. Post-hoc Tukey's test on factor paw found bilateral forelimb use during landings to be significantly greater than ipsilateral forelimb use in landings across all stimulation patterns in intact animals ($p = 0.032$). Two-way repeated measures ANOVA performed on intact ($n = 8$) vs. 6-OHDA treated ($n = 3$) animal baseline performance found no significant effect of paw ($p = 0.06$), lesion state ($p = 0.87$), or paw x lesion state ($p = 0.45$). Two-way repeated measures ANOVA performed on 6-OHDA treated ($n = 3$) animal data found no significant effect of paw ($p = 0.07$), pattern ($p = 0.42$), or paw x pattern ($p = 0.44$) with 130Hz stimulation.

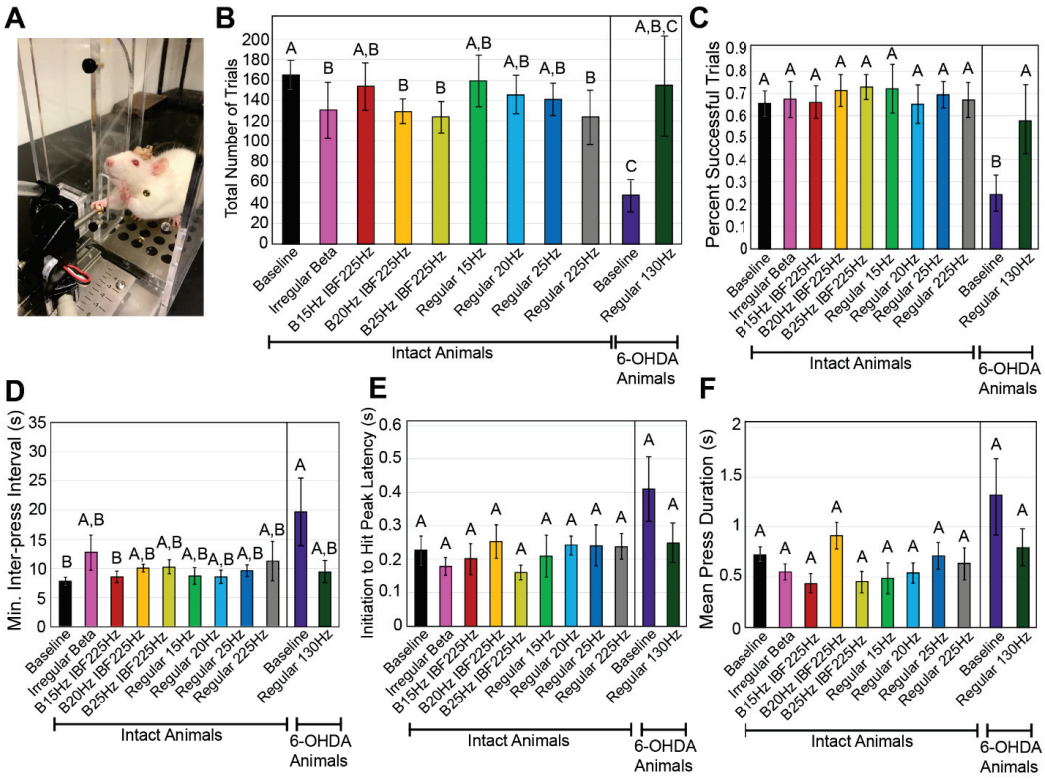

Figure 10. Effect of STN stimulation pattern on performance in the skilled forelimb reaching test. Error bars indicate mean ± SE. Patterns not sharing the same letter are significantly different from each other ($p < 0.05$). **A**: Rat was placed in a clear chamber with a slot to allow it to grasp and depress a lever using only the forelimb contralateral to stimulation or lesioned hemisphere. **B**: Total number of trials per experimental session as a function of stimulation pattern and lesion state. One-way repeated measures ANOVA performed on intact animal data found a significant effect of pattern ($p = 0.0024$). See **Table 1** for *n* for each pattern. Post-hoc Tukey's test on factor pattern found significant differences between baseline and the following patterns: Irregular Beta ($p = 0.044$), B20IBF225 ($p = 0.035$), B25IBF225 ($p = 0.021$), and Regular 225Hz ($p = 0.0025$). One-way unpaired t-test performed on 6-OHDA treated ($n = 4$) animal baseline performance vs. intact animal ($n = 8$) performance found a significant effect of lesion state ($p = 0.0003$). One-way matched pairs t-test performed on 6-OHDA treated animal data with ($n = 3$) and without ($n = 3$) 130Hz stimulation found a near significant effect of stimulation ($p = 0.11$). **C**: Percent of trials

resulting in pellet dispensation as a function of stimulation pattern and lesion state. One-way repeated measures ANOVA performed on intact animal data found no significant effect of pattern ($p = 0.30$). See **Table 1** for *n* for each pattern. One-way unpaired t-test performed on 6-OHDA treated ($n = 4$) animal baseline performance vs. intact animal ($n = 8$) performance found a significant effect of lesion state ($p = 0.0025$). One-way matched pairs t-test performed on 6-OHDA treated animal data with ($n = 3$) and without ($n = 3$) 130Hz stimulation found a significant effect of 130Hz stimulation ($p = 0.017$). **D**: Minimum inter-press interval as a function of stimulation pattern and lesion state. One-way repeated measures ANOVA performed on intact animal data found no significant effect of pattern ($p = 0.21$). See **Table 1** for *n* for each pattern. One-way unpaired t-test performed on 6-OHDA treated ($n = 4$) animal baseline performance vs. intact animal ($n = 8$) performance found a significant effect of lesion state ($p = 0.041$). One-way matched pairs t-test performed on 6-OHDA treated animal data with ($n = 3$) and without ($n = 3$) 130Hz stimulation found no significant effect of 130Hz stimulation ($p = 0.24$). **E**: Initiation to hit peak latency as a function of stimulation pattern and lesion state. One-way performed on intact animal data found no significant effect of pattern ($p = 0.44$). See **Table 1** for *n* for each pattern. One-way unpaired t-test performed on 6-OHDA treated ($n = 4$) animal baseline performance vs. intact animal ($n = 8$) performance found a near significant effect of lesion state ($p = 0.07$). One-way matched pairs t-test performed on 6-OHDA treated animal data with ($n = 3$) and without ($n = 3$) 130Hz stimulation found no significant effect of 130Hz stimulation ($p = 0.17$). **F**: Mean press duration as a function of stimulation pattern and lesion state. One-way repeated measures ANOVA performed on intact animal data found a significant effect of pattern ($p = 0.037$), but post-hoc Tukey's test found no significant differences among patterns. See **Table 1** for *n* for each pattern. One-way unpaired t-test performed on 6-OHDA treated ($n = 4$) animal baseline performance vs. intact animal ($n = 8$) performance found a near significant effect of lesion state ($p = 0.15$). One-way matched pairs t-test performed on 6-OHDA treated animal data with ($n = 3$) and without ($n = 3$) 130Hz stimulation found no significant effect of 130Hz stimulation ($p = 0.20$).

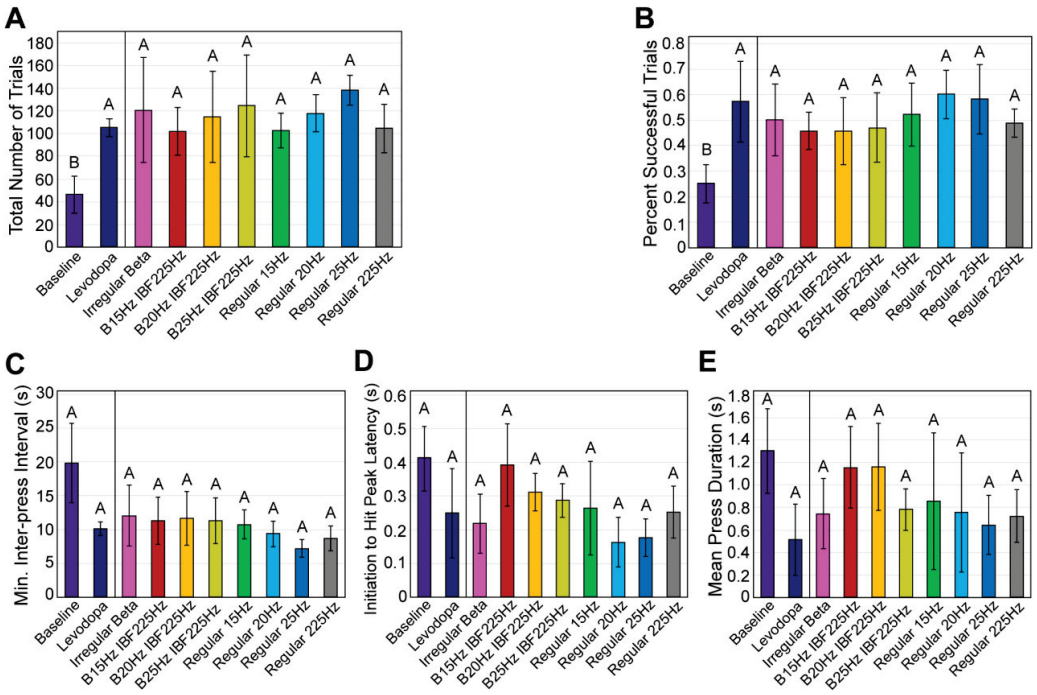

Figure 11. Effect of STN stimulation pattern on performance by levodopa-treated 6-OHDA rats in the skilled forelimb reaching test. Error bars indicate mean ± SE. Patterns not sharing the same letter are significantly different from each other ($p < 0.05$). See **Table 1** for *n* for each pattern. **A:** Total number of trials per experimental session as a function of stimulation pattern and drug condition. One-way matched pairs t-test performed on 6-OHDA treated animal baseline performance without stimulation or levodopa ($n = 3$) vs. with levodopa ($n = 3$) found a significant effect of drug ($p = 0.026$). One-way repeated measures ANOVA performed levodopa-treated 6-OHDA animal performance found no significant effect of stimulation pattern ($p = 0.92$). **B:** Percent of trials resulting in pellet dispensation as a function of stimulation pattern and drug condition. One-way matched pairs t-test performed on 6-OHDA treated animal baseline performance without stimulation or levodopa ($n = 3$) vs. with levodopa ($n = 3$) found a significant effect of drug ($p = 0.016$). One-way repeated measures ANOVA performed on levodopa-treated 6-OHDA animal performance found no significant effect of stimulation pattern ($p = 0.58$). **C:** Minimum inter-press interval as a function of stimulation pattern and drug condition. One-way matched pairs t-test performed on 6-OHDA treated animal baseline performance without stimulation or levodopa (*n*

= 3) vs. with levodopa (*n* = 3) found no significant effect of drug (p = 0.24). One-way repeated measures ANOVA performed on levodopa-treated 6-OHDA animal performance found no significant effect of stimulation pattern (p = 0.42). **D:** Initiation to hit peak latency as a function of stimulation pattern and drug condition. One-way matched pairs t-test performed on 6-OHDA treated animal baseline performance without stimulation or levodopa (*n* = 3) vs. with levodopa (*n* = 3) found no significant effect of drug (p = 0.16). One-way repeated measures ANOVA performed on levodopa-treated 6-OHDA animal performance found no significant effect of stimulation pattern (p = 0.36). **E:** Mean press duration as a function of stimulation pattern and drug condition. One-way matched pairs t-test performed on 6-OHDA treated animal baseline performance without stimulation or levodopa (*n* = 3) vs. with levodopa (*n* = 3) found no significant effect of drug (p = 0.15). One-way repeated measures ANOVA performed on levodopa-treated 6-OHDA animal performance found no significant effect of stimulation pattern (p = 0.44).

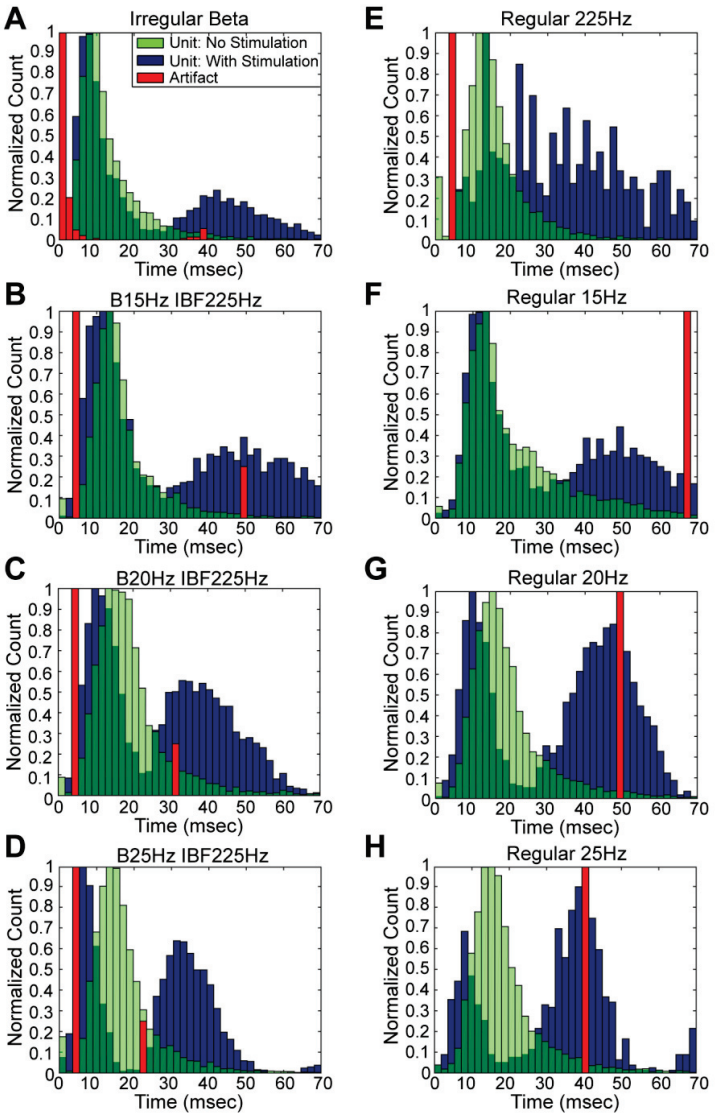

1405

1406 **Figure 12.** Effect of STN stimulation patterns on single unit ISI histograms. **A-H**: Normalized histograms

1407 for a representative SNr unit representing the pre-stimulation and stimulation periods. Stimulation causes

1408 a shift in the unit ISI histogram to mimic the artifact IPI histogram.

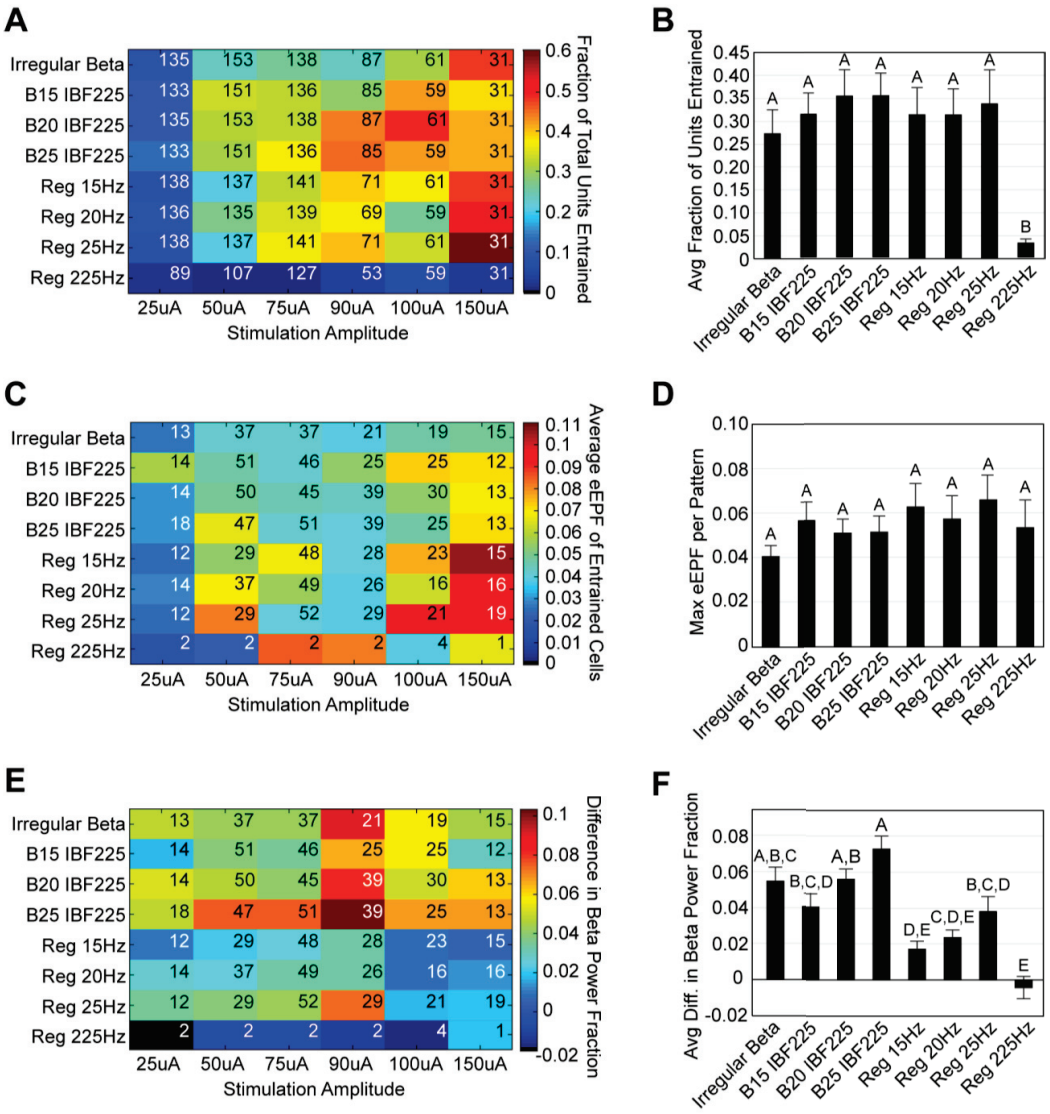

Figure 13. Effect of STN stimulation patterns on excitatory effective pulse fraction. Patterns not connected by the same letter are significantly different from each other ($p < 0.05$). Error bars indicate mean ± SE. **A**: Fraction of total SNr units entrained as a function of stimulation pattern and amplitude. Inset numbers refer to total number of units assessed (*n*) per stimulation pattern and amplitude setting. Two-way ANOVA performed on entrainment fractions found a significant effect of pattern ($p < 0.0001$), amplitude ($p < 0.0001$), and pattern x amplitude ($p = 0.030$). **B**: Post-hoc Tukey's test results for factor

pattern across amplitude for entrainment fraction ANOVA. Post-hoc Tukey's testing showed a significant difference between Regular 225 Hz and all other patterns ($p < 0.0001$ for all comparisons); all other patterns were equivocal in degree of entrainment. **C**: Average eEPF of entrained SNr units as a function of stimulation pattern and amplitude. Inset numbers refer to total number of entrained units (*n*) included in the calculation. Two-way ANOVA found a significant effect of amplitude ($p < 0.0001$), but no significant effect of pattern ($p = 0.43$) or pattern x amplitude ($p = 0.69$). **D**: Post-hoc Tukey's test results for factor pattern across amplitude for average eEPF value. No significant differences across pattern were found ($p < 0.05$). **E**: Difference in beta power fraction between stimulation and pre-stimulation power spectra as a function of stimulation pattern and amplitude. Inset numbers refer to total number of entrained units (*n*) included in the calculation. Two-way ANOVA found a significant effect of pattern ($p < 0.0001$), but no significant effect of amplitude ($p = 0.54$) or pattern x amplitude ($p = 0.82$). **F**: Post-hoc Tukey's test results for factor pattern across amplitude for difference in beta power ANOVA. Post-hoc Tukey's testing showed a multiple significant differences between bursting patterns and continuous frequency patterns ($p < 0.05$).

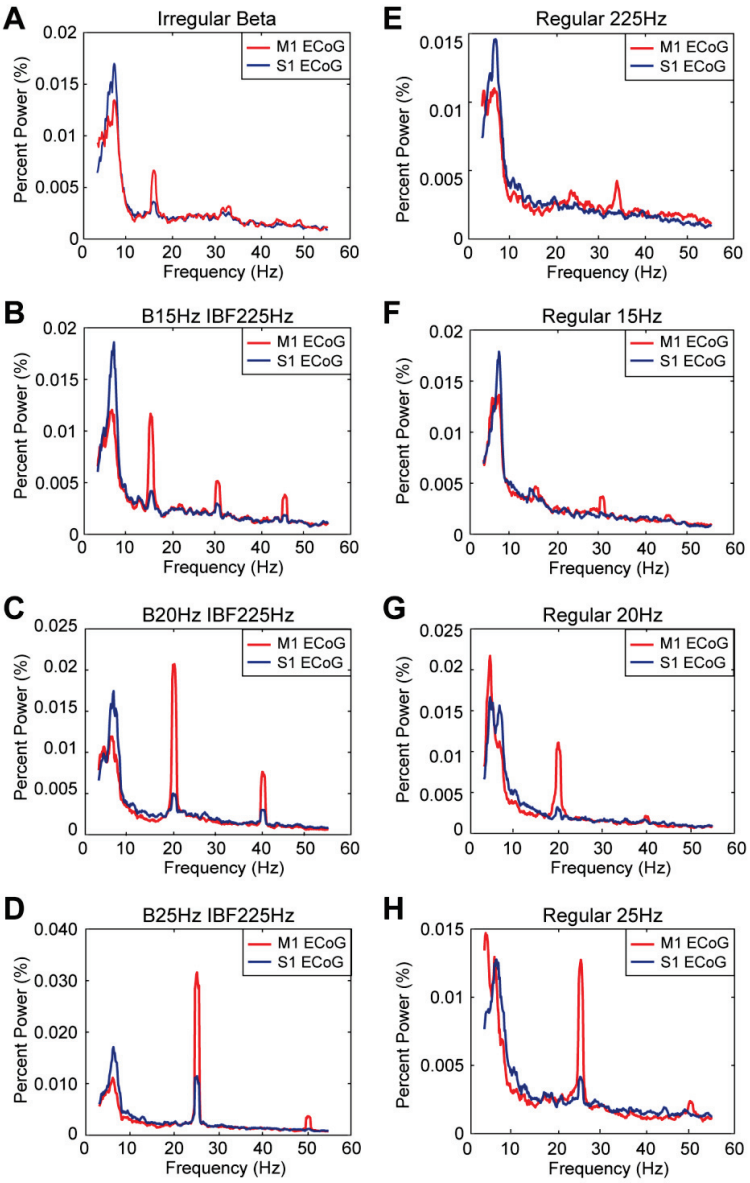

Figure 14. Effect of STN stimulation patterns on ipsilateral M1 and contralateral S1 ECoG. **A-H:** Multi-taper spectra normalized to percent of total power for a representative animal across stimulation patterns at the maximum stimulation amplitude for that animal.

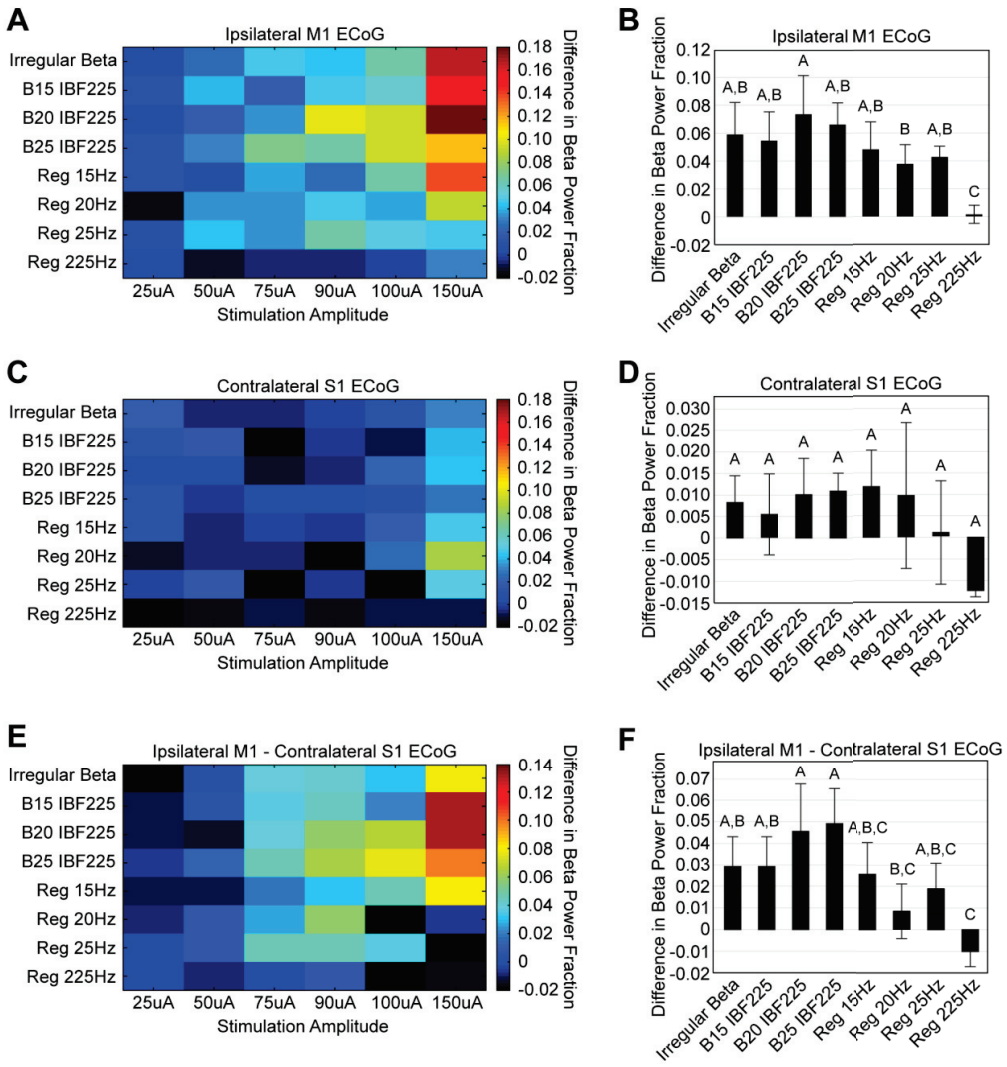

Figure 15. Effect of STN stimulation patterns on ipsilateral M1 and contralateral S1 ECoG. ECoG data from *n* = 10 rats were analyzed. Patterns not sharing the same letter are significantly different from each other ($p < 0.05$). Error bars indicate mean ± SE. **A:** Difference in beta power fraction between ipsilateral M1 ECoG during stimulation and ipsilateral M1 ECoG prior to stimulation. Two-way ANOVA performed on the difference in beta power fraction found a significant effect of pattern ($p < 0.0001$), amplitude ($p < 0.0001$), and pattern x amplitude ($p = 0.0004$). **B:** Post-hoc Tukey's test results for factor pattern across amplitude for difference in beta power fraction for ipsilateral M1 ECoG. A significant difference was found

between B20 IBF225Hz and Regular 20Hz stimulation ($p = 0.04$). All patterns were significantly different from Regular 225Hz stimulation. **C:** Difference in beta power fraction between contralateral S1 ECoG during stimulation and contralateral S1 ECoG prior to stimulation. Two-way ANOVA performed on the difference in beta power fraction found a significant effect of amplitude ($p = 0.0008$) but no significant effects of pattern ($p = 0.49$) or pattern x amplitude ($p = 0.46$). **D:** Post-hoc Tukey's test results for factor pattern across amplitude for difference in beta power fraction for contralateral S1 ECoG. No statistically significant differences across pattern were found ($p < 0.05$). **E:** Difference in beta power fraction between ipsilateral M1 ECoG and contralateral S1 ECoG. Two-way ANOVA found a significant effect of pattern ($p = 0.0002$), amplitude ($p < 0.0001$), and pattern x amplitude ($p < 0.0001$). **F:** Post-hoc Tukey's test for factor pattern across amplitude for difference in beta power fraction between ipsilateral M1 ECoG and contralateral S1 ECoG. Multiple significant differences were found between burst patterns and some continuous frequency patterns ($p < 0.05$).

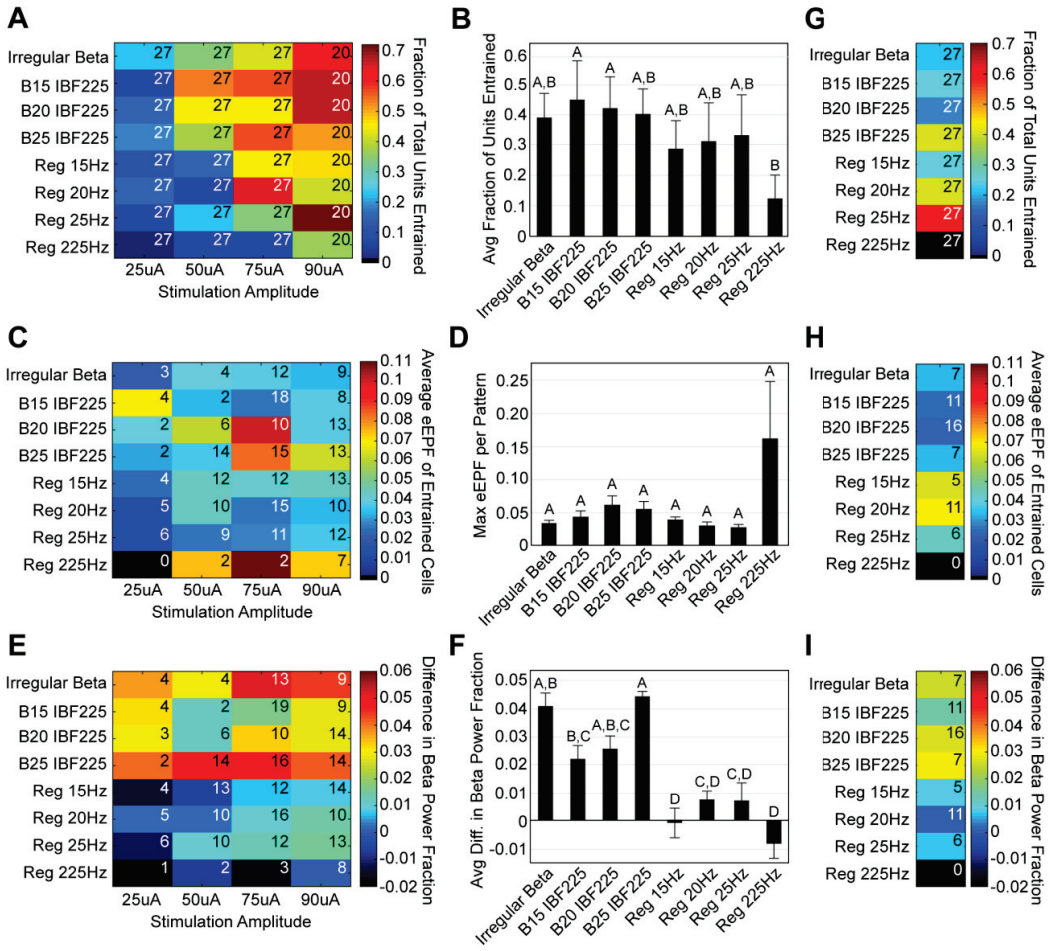

Figure 16. Effect of STN stimulation patterns on excitatory effective pulse fraction in 6-OHDA treated animals. Patterns not sharing the same letter are significantly different from each other ($p < 0.05$). Error bars indicate mean ± SE. **A**: Fraction of total SNr units entrained as a function of stimulation pattern and amplitude in 6-OHDA-lesioned animals not pre-treated with levodopa. Inset numbers refer to total number of units assessed (*n*) per stimulation pattern and amplitude setting. Two-way ANOVA performed on entrainment fractions found a significant effect of pattern ($p = 0.032$) and amplitude ($p < 0.0001$), but no significant pattern x amplitude interaction ($p = 0.91$). **B**: Post-hoc Tukey's test results for factor pattern for entrainment fraction ANOVA in 6-OHDA-lesioned animals not pre-treated with levodopa. Statistically significant differences between Regular 225Hz and B15IBF225/B20IBF225 was found ($p < 0.05$). **C**:

Average eEPF of entrained SNr units as a function of stimulation pattern and amplitude in 6-OHDA-lesioned animals not pre-treated with levodopa. Inset numbers refer to total number of entrained units (*n*) included in the calculation. Two-way ANOVA found no significant effect of amplitude ($p = 0.52$), pattern ($p = 0.35$), or pattern x amplitude ($p = 0.99$). **D**: Post-hoc Tukey's test results for factor pattern for average eEPF value in 6-OHDA-lesioned animals not pre-treated with levodopa. No significant differences were found among patterns ($p < 0.05$). **E**: Difference in beta power fraction between stimulation and pre-stimulation power spectra as a function of stimulation pattern and amplitude in 6-OHDA-lesioned animals not pre-treated with levodopa. Inset numbers refer to total number of entrained units (*n*) included in the calculation. Two-way ANOVA found a significant effect of pattern ($p < 0.0001$) and amplitude ($p = 0.021$) but no significant pattern x amplitude interaction ($p = 0.53$). **F**: Post-hoc Tukey's test results for factor pattern for difference in beta power ANOVA. Patterns not connected by the same letter are significantly different from each other ($p < 0.05$). **G:** Fraction of total SNr units entrained as a function of stimulation pattern in 6-OHDA-lesioned animals pre-treated with levodopa. Inset numbers refer to total number of units assessed (*n*) per stimulation pattern and amplitude setting. Two-way ANOVA comparing entrainment fraction with levodopa pre-treatment to the average of the entrainment fractions without levodopa at 75uA and 90uA (**A**) found a significant effect of drug ($p = 0.023$) but no significant effect of pattern ($p = 0.65$) or drug x pattern ($p = 0.60$). Post-hoc Student's t-test revealed a greater fraction of units entrained without levodopa than with the application of levodopa ($p = 0.023$). **H:** Average eEPF of entrained SNr units as a function of stimulation pattern in 6-OHDA-lesioned animals pre-treated with levodopa. Inset numbers refer to total number of entrained units (*n*) included in the calculation. Two-way ANOVA comparing average eEPF with levodopa pre-treatment to the average of eEPF values without levodopa at 75uA and 90uA (**B**) found no effect of drug ($p = 0.69$), pattern ($p = 0.64$), or drug x pattern ($p = 0.19$). **I:** Difference in beta power fraction between stimulation and pre-stimulation power spectra as a function of stimulation pattern in 6-OHDA-lesioned animals pre-treated with levodopa. Inset numbers refer to total number of entrained units (*n*) included in the calculation. Two-way ANOVA comparing average difference in beta power fraction with levodopa to the average difference in beta power fraction without levodopa at 75uA and 90uA (**C**) found a significant effect of drug ($p = 0.0021$), and pattern ($p = 0.0002$), but no significant pattern x drug interaction ($p = 0.18$). Post-hoc Student's t-test for factor drug found a

smaller increase in beta power fraction with levodopa than without levodopa ($p = 0.0021$). Post-hoc Tukey's test for factor pattern found that beta-patterned paradigms, particularly B25 IBF225, B20 IBF225, and GA Beta patterns, were superior to increasing beta power fraction than low frequency control patterns.

Table 1. Stimulation patterns tested in model simulations, healthy (intact) animals, and 6-OHDA treated animals.

Pattern	Model	Bar Test	Open Field Test	Adjusting Steps Test	Forelimb Use Asymmetry Test	Skilled Forelimb Reaching Test
		Intact Animals				
No Stimulation	X	7	9	8	5	8
Irregular Beta	X	5	5	7	5	5
B15 IBF225	X	5	6	7	3	6
B20 IBF225	X	5	5	5		5
B25 IBF225	X	5	6	7	3	6
Regular 15Hz	X	7	8	6	3	5
Regular 20Hz	X	5	5	5		5
Regular 25Hz	X	5	6	7		6
Regular 225Hz	X	7	9	7	3	5
		6-OHDA Treated Animals				
No Stimulation	X	9	5	6	3	4
Regular 130Hz		9	5	3	3	3
		6-OHDA Levodopa + Stimulation Experiments				
Levodopa (LD)				3		3
LD + Irregular Beta				3		3
LD + B15 IBF225				3		3
LD + B20 IBF225				3		3
LD + B25 IBF225				3		3
LD + Regular 15Hz				3		3
LD + Regular 20Hz				3		3
LD + Regular 25Hz				3		3
LD + Regular 225Hz				3		3

Table 2. Two-way ANOVA of the effects of beta-patterned stimulation and fraction of total cells activated on the amount of beta band power in the 'healthy' biophysical circuit model of the cortico-basal ganglia-thalamic loop.

Parameter	p-value	*F*	df
Stimulation pattern	< 0.0001	1118.4	9, 34.7
Log(fraction of total cells activated)	< 0.0001	729.3	1, 2.51
Interaction term	< 0.0001	314.0	9, 9.73

Table 3. Bar test: Results of statistical analyses for effects on length of time on bar.

Parameter	n/group	Test Statistic	df	p-value
Intact Animals				
	Two-way RMANOVA (*F*)			
Stimulation Pattern	See Table 1	0.40	8, 36.1	0.92
Paw		1.06	1, 6.9	0.34
Interaction term		0.64	8, 38.2	0.74
6-OHDA Lesioned Animals				
	Wilcoxon rank sum (χ^2)			
Effect of 6-OHDA toxin	9 vs. 7	15.8	1	< 0.0001
Effect of 130Hz stim after lesion	9/group	16.5	1	< 0.0001

Table 4. Open field test: Results of statistical analyses for effects on locomotor activity.

Metric	Parameter	n/group	Test Statistic	df	p-value
Intact Animals					
		One-way RMANOVA (*F*)			
Linear speed	Stimulation Pattern	See Table 1	1.60	8, 42.7	0.15
Pauses per second	Stimulation Pattern		1.58	8, 42.6	0.16
Pause length	Stimulation Pattern		1.01	8, 45.2	0.44
6-OHDA Lesioned Animals					
		Unpaired t-test (*T*)			
Linear speed	6-OHDA toxin effect	5 vs. 9	0.36	6.5	0.73
Pauses per second	6-OHDA toxin effect		-1.75	11.4	0.11
Pause length	6-OHDA toxin effect		-1.49	9.9	0.17
		Paired t-test (*T*)			
Linear speed	130Hz stim after lesion	5/group	0.67	4	0.54
Pauses per second	130Hz stim after lesion		-1.47	4	0.22
Pause length	130Hz stim after lesion		1.19	4	0.30

Table 5. Adjusting steps test: Results of statistical analyses for effects on number of steps.

Parameter	n/group	Test Statistic	df	p-value
Intact Animals				
	Two-way RMANOVA (*F*)			
Stimulation pattern	See Table 1	0.96	8, 35.6	0.48
Paw		1.38	1, 7.72	0.28
Interaction term		1.83	8, 36.9	0.10
6-OHDA Lesioned Animals				
	Two-way RMANOVA (*F*)			
6-OHDA toxin	8 vs. 6	4.91	1, 10.5	0.0498
Paw		26.5	1, 1.93	0.039
Interaction term		22.9	1, 10.1	0.0007
	Two-way RMANOVA (*F*)			
130Hz stimulation	8 vs. 6	40.6	1, 2.21	0.019
Paw		17.0	1, 3.14	0.024
Interaction term		1.06	1, 2.74	0.38
	Unpaired t-test (*T*)			
Levodopa effect on contralateral paw	6 vs. 3	-7.78	6.63	0.0001
6-OHDA Lesioned Animals + Levodopa				
	Two-way RMANOVA (*F*)			
Stimulation pattern	See Table 1	1.31	8, 16	0.31
Paw		8.37	1, 2	0.10
Interaction term		1.89	8, 16	0.13

Table 6. Forelimb use asymmetry test: Results of statistical analyses for effects on forelimb akinesia.

Metric	Parameter	n/group	Test Statistic	df	p-value
Intact Animals					
		Two-way RMANOVA (*F*)			
Number of Touches (Vertical)	Stimulation Pattern	See Table 1	0.84	5, 11.1	0.55
	Paw		5.09	2, 11.5	0.026
	Interaction		0.69	10, 21.5	0.72
Number of Landings	Stimulation Pattern	See Table 1	1.13	5, 63.8	0.36
	Paw		4.21	2, 95.6	0.021
	Interaction		1.19	10, 136	0.32
6-OHDA Lesioned Animals					
		Two-way RMANOVA (*F*)			
Number of Touches (Vertical)	6-OHDA toxin effect	8 vs. 3	0.0004	1, 0.002	0.98
	Paw		2.52	2, 23.83	0.10
	Interaction		1.14	2, 10.72	0.34
Number of Touches (Vertical)	130Hz stim after lesion	3/group	1.00	1, 2	0.42
	Paw		0.74	2, 4	0.53
	Interaction		1.00	2, 4	0.44
		Two-way RMANOVA (*F*)			
Number of Landings	6-OHDA toxin effect	8 vs. 3	0.027	1, 6	0.87
	Paw		3.65	2, 12	0.06
	Interaction		0.85	2, 12	0.45
Number of Landings	130Hz stim after lesion	3/group	1.00	1, 2	0.42
	Paw		5.45	2, 4	0.07
	Interaction		1.00	2, 4	0.44

Table 7. Skilled Forelimb Reaching Test: Results of statistical analyses for effects on forelimb bradykinesia.

Metric	Parameter	n/group	Test Statistic	df	p-value
Intact Animals					
		One-way RMANOVA (*F*)			
Total trials attempted	Stim Pattern	See Table 1	3.77	8, 38.5	0.0024
% Successful Trials	Stim Pattern		1.28	8, 23.5	0.30
Minimum Inter-press Interval	Stim Pattern		1.43	8, 43.6	0.21
Initiation to Hit Peak Latency	Stim Pattern		1.06	8, 43.6	0.44
Mean Press Duration	Stim Pattern		2.62	8, 20.6	0.037
6-OHDA Lesioned Animals					
		Unpaired t-test (*T*)			
Total trials attempted	6-OHDA toxin	4 vs. 8	-5.63	7.46	0.0003
% Successful Trials	6-OHDA toxin		-4.13	6.61	0.0025
Minimum Inter-press Interval	6-OHDA toxin		2.40	3.57	0.041
Initiation to Hit Peak Latency	6-OHDA toxin		1.80	4.35	0.07
Mean Press Duration	6-OHDA toxin		1.23	3.58	0.15
		One-way matched pairs t-test (*T*)			
Total trials attempted	130Hz stim	3/group	1.76	2	0.11
% Successful Trials	130Hz stim		5.31	2	0.017
Minimum Inter-press Interval	130Hz stim		-0.86	2	0.24
Initiation to Hit Peak Latency	130Hz stim		-1.24	2	0.17
Mean Press Duration	130Hz stim		-1.05	2	0.20
		One-way matched pairs t-test (*T*)			
Total trials attempted	Levodopa	3/group	4.20	2	0.026
% Successful Trials	Levodopa		5.51	2	0.016
Minimum Inter-press Interval	Levodopa		-0.84	2	0.24
Initiation to Hit Peak Latency	Levodopa		-1.32	2	0.16
Mean Press Duration	Levodopa		-1.71	2	0.11
6-OHDA Lesioned Animals + Levodopa					
		One-way RMANOVA (*F*)			
Total trials attempted	Stim Pattern	See Table 1	0.38	8, 16	0.92
% Successful Trials	Stim Pattern		0.84	8, 16	0.58
Minimum Inter-press Interval	Stim Pattern		1.09	8, 16	0.42
Initiation to Hit Peak Latency	Stim Pattern		1.19	8, 16	0.36
Mean Press Duration	Stim Pattern		1.05	8, 16	0.44

Table 8. Effect of STN stimulation patterns on SNr unit entrainment: Results of statistical analyses for effects on SNr units in intact, 6-OHDA lesioned, and 6-OHDA lesioned + levodopa treated animals. eEPF = excitatory Effective Pulse Fraction. BPF = Beta power fraction.

Metric	Parameter	n/group	Test Statistic	df	p-value
SNr units in Intact Animals (Pre-6-OHDA)					
			Two-way ANOVA (*F*)		
Entrainment fraction	Amplitude	See **Figure 13A inset**	100.1	1, 0.44	< 0.0001
	Stim Pattern		15.2	7, 0.47	< 0.0001
	Interaction		2.61	7, 0.08	0.03
Average eEPF	Amplitude	See **Figure 13C inset**	25.8	1, 0.008	< 0.0001
	Stim Pattern		1.03	7, 0.002	0.43
	Interaction		0.68	7, 0.001	0.69
Difference in BPF	Amplitude	See **Figure 13E inset**	0.38	1, 0.0001	0.54
	Stim Pattern		11.9	7, 0.024	< 0.0001
	Interaction		0.50	7, 0.001	0.82
SNr units in Post-6-OHDA Lesioned Animals					
			Two-way ANOVA (*F*)		
Entrainment fraction	Amplitude	See **Figure 16A inset**	56.4	1, 0.80	< 0.0001
	Stim Pattern		3.03	7, 0.30	0.03
	Interaction		0.36	7, 0.036	0.91
Average eEPF	Amplitude	See **Figure 16C inset**	0.43	1, 0.001	0.52
	Stim Pattern		1.22	7, 0.027	0.35
	Interaction		0.10	7, 0.002	0.99
Difference in BPF	Amplitude	See **Figure 16E inset**	6.63	1, 0.0004	0.02
	Stim Pattern		19.7	7, 0.009	< 0.0001
	Interaction		0.91	7, 0.0004	0.53
SNr units in Post-6-OHDA Lesioned Animals + Levodopa					
			Two-way ANOVA (*F*)		
Entrainment fraction	Drug state	See **Figure 16G inset**	8.43	1, 0.17	0.023
	Stim Pattern		0.72	6, 0.086	0.65
	Interaction		0.80	6, 0.096	0.60
Average eEPF	Drug state	See **Figure 16H inset**	0.17	1, 5.6e-5	0.69
	Stim Pattern		0.73	6, 0.001	0.64
	Interaction		2.04	6, 0.004	0.19
Difference in BPF	Drug state	See **Figure 16I inset**	22.47	1, 0.0004	0.0021
	Stim Pattern		24.21	6, 0.003	0.0002
	Interaction		2.07	6, 0.0002	0.18

Table 9. Effect of STN stimulation patterns on ECoG activity: Results of statistical analyses for effects on ipsilateral M1 and contralateral S1 ECoG. BPF = Beta Power Fraction.

Metric	Parameter	n/group	Test Statistic	df	p-value
Ipsilateral M1 ECoG					
		Two-way ANOVA (*F*)			
Difference in BPF	Amplitude	n = 10	161.7	1, 0.056	< 0.0001
	Stim Pattern		8.50	7, 0.020	< 0.0001
	Interaction		5.28	7, 0.013	0.0004
Contralateral S1 ECoG					
		Two-way ANOVA (*F*)			
Difference in BPF	Amplitude	n = 10	13.7	1, 0.006	0.0008
	Stim Pattern		0.95	7, 0.003	0.49
	Interaction		0.99	7, 0.003	0.46
Ipsilateral M1 ECoG - Contralateral S1 ECoG					
		Two-way ANOVA (*F*)			
Difference in BPF	Amplitude	n = 10	52.0	1, 0.019	< 0.0001
	Stim Pattern		5.84	7, 0.015	0.0002
	Interaction		7.25	7, 0.019	< 0.0001